Generalized nonlinear sector approaches for Takagi-Sugeno models

Gustave Bainier, Benoît Marx, Jean-Christophe Ponsart

Generalized Nonlinear Sector Approaches for Takagi-Sugeno Models

Gustave Bainier[a,*], Benoît Marx[a], Jean-Christophe Ponsart[a]

[a] *Université de Lorraine, CNRS, CRAN, F54000 Nancy, France,*

Abstract

The Nonlinear Sector Approach (NLSA) is a way to construct Takagi-Sugeno (T-S) models which exactly represent nonlinear systems with bounded nonlinearities. Generally, the nonlinearities are bounded by a box-shaped set, however, this paper generalizes the NLSA for polytopic and smooth convex bounding sets, providing new ways of reducing the intrinsic conservatism of T-S representations with interdependent scheduling parameters. Some Linear Matrix Inequalities (LMI) criteria for stability analysis of these models are provided throughout the paper.

Keywords: Takagi-Sugeno Model, Nonlinear Sector Approach, Linear Matrix Inequality, Quadratic Lyapunov Function

1. Introduction

The study of nonlinear systems for control purposes is a challenging task that has received a great amount of attention in the last century due to its numerous applications in the fields of engineering [1], biology [2] or even economics and finance [3, 4]. A nonlinear dynamical system is typically given by the following equations

$$\delta x(t) = f(x(t), u(t), \sigma(t), t) \tag{1a}$$
$$y(t) = g(x(t), u(t), \sigma(t), t) \tag{1b}$$

where $x(t) \in \mathbb{R}^{n_x}$, $u(t) \in \mathbb{R}^{n_u}$ and $y(t) \in \mathbb{R}^{n_y}$ are the state, input and output vector of the system respectively; $\sigma(t) \in \mathbb{R}^{n_\sigma}$ is a vector of exogenous signals (such as noise); f and g are two (generally smooth) nonlinear functions; and δ is the shift operator, with $\delta x(t) = \dot{x}(t)$ in the continuous-time case (and $t \in \mathbb{R}$) or $\delta x(t) = x(t+1)$ in the discrete-time case (and $t \in \mathbb{Z}$). These systems are generally implicitly assumed to have a solution for "all time", in the sense that given an initial condition $x(t_0) \in \mathbb{R}^{n_x}$, the trajectory $x(t)$ is uniquely defined on the maximal interval of existence $[t_0, +\infty)$. Several models have been suggested by the literature to offer a systematic approach to the control synthesis of such systems. Among them, a recurring idea consists in approximating or rewriting the shifted state vector $\delta x(t)$ and the output $y(t)$ as a weighted sum of several Linear Time Invariant (LTI) systems, the so-called local models (or submodels), to obtain:

$$\delta x(t) = \sum_{i=1}^{n_\Omega} h_i(\theta) \left[A_i x(t) + B_i u(t) + \alpha_i\right] \tag{2a}$$
$$y(t) = \sum_{i=1}^{n_\Omega} h_i(\theta) \left[C_i x(t) + D_i u(t) + \beta_i\right] \tag{2b}$$

with n_Ω the number of local models; $\theta \in \Omega \subseteq \mathbb{R}^{n_\theta}$ a vector of scheduling parameters which usually depend on $x(t)$, $u(t)$, $\sigma(t)$ and t; $\alpha_i \in \mathbb{R}^{n_x}$ and $\beta_i \in \mathbb{R}^{n_y}$ the two affine biases of the i-th local model; and $(h_1, \ldots, h_{n_\Omega})$

*Corresponding author
Email address: gustave.bainier@univ-lorraine.fr (Gustave Bainier)

the weighting functions, also known as the membership functions or the activation functions (indeed, h_i provides the weight of the i-th local model of the system). Several terminologies are employed in the literature to refer to this kind of model:

- the Takagi-Sugeno (fuzzy) model (T-S) [5];
- the multiple model [6];
- the polytopic (quasi-)Linear Parameter Varying (LPV) model [7];
- the linear polytopic model [8].

In particular, the "quasi-LPV" terminology is reserved for cases when θ depends on the state $x(t)$, whereas the "linear polytopic model" terminology is reserved for cases when θ does not depend on the state $x(t)$ [9]. Moreover, as a special case, (2) is also equivalent to a flattened tensor-product model [10], to a polynomial fuzzy model with only linear terms [11], or to a polytopic linear differential inclusion model with known weights [12]. The weighting functions $(h_1, \dots, h_{n_\Omega})$ satisfy the convex sum properties:

$$h_i(\theta) \geq 0 \qquad \text{[positivity]} \tag{3}$$

$$\sum_{i=1}^{n_\Omega} h_i(\theta) = 1 \qquad \text{[partition of unity]} \tag{4}$$

Thanks to the convex nature of these models, many control problems with no simple analytical solution can be numerically solved through convex optimization techniques, in particular by formulating them using Linear Matrix Inequalities (LMI) [12, 13, 14].

Two main approaches exist in the literature to obtain a T-S model from a nonlinear system: numerical identification using measurements of the system behavior, or analytical construction using an already existing nonlinear model of the system dynamic. The first approach is out of the scope of this paper and the interested reader is referred to [15, 16, 17, 18, 19, 20, 21]. Common examples of the second approach are the dynamic linearization at different representative points of the system [22], the use of unimodal basis functions with arbitrary accuracy on the approximation error [23], and the Nonlinear Sector Approach (NLSA) [24, 25], also called the convex polytopic transformation [26]. The latter is the most prominent in the literature of T-S models, since it provides an exact representation of the initial nonlinear system on a box-shaped set of the scheduling parameter space. Formally for all θ in the box-shaped set Ω:

$$\begin{cases} \sum_{i=1}^{n_\Omega} h_i(\theta(x,u,\sigma,t)) \left[A_i x + B_i u + \alpha_i\right] = f(x,u,\sigma,t) \\ \sum_{i=1}^{n_\Omega} h_i(\theta(x,u,\sigma,t)) \left[C_i x + D_i u + \beta_i\right] = g(x,u,\sigma,t) \end{cases} \qquad \text{[exactness]} \tag{5}$$

As a matter of fact, this exactness is explained by a third property respected by the weighting functions produced by the NLSA:

$$\sum_{i=1}^{n_\Omega} h_i(\theta_\mathcal{V})\mathcal{V}_i = \mathcal{V} \qquad \text{[linear precision]} \tag{6}$$

This linear precision property states that given a vector $\mathcal{V}$ in the convex hull of $\{\mathcal{V}_1, \dots, \mathcal{V}_{n_\Omega}\}$, weighting each vertex $\mathcal{V}_i$ by $h_i(\theta_\mathcal{V})$ yields back $\mathcal{V}$, with $\theta_\mathcal{V}$ the value of the scheduling parameter at $\mathcal{V}$ [27]. Linear precision makes $(h_1, \dots, h_{n_\Omega})$ the exact barycentric coordinates of the initial nonlinear system within the convex hull of the local LTI models.

Despite its popularity, the NLSA is subject to some key issues: regarding the number of local models needed, which grows exponentially with the dimension of the scheduling parameter space ($n_\Omega = 2^{n_\theta}$) [28], and regarding the intrinsic conservatism of the model. Indeed, modeling a nonlinear system with the convex-sum (2) generally creates a loss of information on the properties of the nonlinearities of the system (such as their interdependence, periodicity, etc), which limits the number of solutions in the optimization problems

obtained with a T-S model-based approach to nonlinear control questions. Some mitigating solutions to these modeling issues have been suggested, for example by using a polar coordinate T-S model [29], by generalizing the NLSA for polynomial fuzzy models [30], by using model reduction schemes [31, 32, 33, 34], or simply by carefully choosing the scheduling parameters of the model [35, 36]. However, most of the conservatism reductions in the literature are performed a-posteriori, that is to say after the construction of the T-S model with its $n_\Omega = 2^{n_\theta}$ local models. The conservatism reduction is usually achieved by using nonquadratric Lyapunov function in the stability analysis of the system [37, 38, 39, 40, 41], and by finding a sharp LMI formulation of the control problem at hand [42, 43, 44, 45, 46, 47]. In particular, one way of sharpening the resulting LMI problems consists in getting rid of some useless vertices of the T-S model, by leveraging the interdependencies of the scheduling parameters [48]. However, if these vertices were in fact useless, one could wonder why they were considered in the NLSA in the first place.

The authors argue that the key issues of the NLSA could be addressed by acknowledging that the box-shaped bounding set Ω is ultimately incidental to the approach, and could be replaced by larger classes of convex sets. Somehow, the generalization of the NLSA to simple polytopes (see Definition 4.1) can already be found in the T-S literature [25], but has received very little attention yet, despite its relevance. Flexibility on the convex polytope used to bound the scheduling vector θ is also not uncommon in the polytopic LPV model literature [49, 35, 50]. However, since the generalization of the NLSA to simple polytopes is rarely leveraged in the construction of polytopic LPV models, the explicit expression of the weighting functions is rarely given. This is still a limiting issue in the polytopic LPV framework, in particular for the PDC schemes relying on the real-time calculation of these weights.

This paper presents several convex generalizations of the NLSA which are not discussed in the literature yet, and which can not only reduce the minimal number of local models needed, but can also lead to a reduction of the intrinsic conservatism of some T-S models with interdependent scheduling parameters.

The paper is organized as follows: in Section 2, the notations of the document are introduced. Section 3 provides a generic description of the NLSA and introduces a nonlinear system which is studied numerically in each of the following sections of this paper. Section 4 focuses on the NLSA for polytopic bounding sets, which results in the well-known NLSA [24] when this bounding set is a box, and in the lesser-known generalization of the NLSA when this bounding set is a simple polytope [25]. Section 5 provides similar results for convex bounding sets with a smooth boundary, which results in a generalization of the NLSA for a new kind of T-S models which is not discussed in the literature yet. New stability results are given to study these T-S-like models using simple LMIs. Finally, some conclusions and perspectives are discussed in Section 6.

2. Notations

$\mathbb{Z}$, $\mathbb{N}$ stand resp. for the set of integer and non-negative integers. Given $k, m \in \mathbb{Z}$, $[\![k, m]\!]$ stands for the subset of integers between k and m (both included). Given $a \in \mathbb{N}$, $\overline{a_{[k]} \dots a_{[1]}}^{(b)}$ denotes the standard base-b positional notation of a, where $a_{[i]} \in [\![0, b-1]\!]$ stands for the i-th digit of a, with $b \in [\![2, +\infty[\![$:

$$a = \overline{a_{[k]} \dots a_{[1]}}^{(b)} = \sum_{i=1}^{k} a_{[i]} b^{i-1} \tag{7}$$

$\mathbb{R}$, $\mathbb{R}_{>0}$ stand resp. for the set of real numbers and positive real numbers. $\mathbb{R}^{p\times q}$ denotes the set of matrices of p rows and q columns with coefficients in $\mathbb{R}$. The matrices with one column in $\mathbb{R}^{p\times 1}$ are identified with vectors of $\mathbb{R}^p$. Given a matrix $A \in \mathbb{R}^{p\times q}$ and a vector $v \in \mathbb{R}^p$, $A_{(i,j)}$ stands for the (i,j)-th coefficient of A and $v_{(i)}$ stands for the i-th coordinate of v. $\|\cdot\|$ stands for the Euclidean norm for vectors. $\langle\cdot|\cdot\rangle$ stands for the dot product between two vectors. Given a matrix $E \in \mathbb{R}^{p\times q}$, $E^\top$ denotes its transposition. If $p = q$, then $\mathcal{H}(E) = E^\top + E$. Given two symmetric matrices $E, F \in \mathbb{R}^{p\times p}$, $E \succ F$ means that $E - F$ is positive-definite (which is denoted $E - F \succ 0$) and that $F - E$ is negative-definite ($F - E \prec 0$).

A n-dimensional polytope $\mathcal{P} \subset \mathbb{R}^n$ is defined as the convex hull of a finite set S of vectors of $\mathbb{R}^n$ containing at least $n+1$ affinely independent vectors. This is denoted by $\mathcal{P} = \text{Hull}(S)$. A n-dimensional polytope is

bounded by a finite number of 0-dimensional and $(n-1)$-dimensional faces which are respectively called its vertices and its facets. The set of vertices and the set of facets of $\mathcal{P}$ are respectively denoted by $v(\mathcal{P})$ and $f(\mathcal{P})$. Given a vertex $\mathcal{V}$ of $v(\mathcal{P})$, $\mathrm{ind}(\mathcal{V})$ stands for the set of facets containing $\mathcal{V}$. Given $\mathcal{F}$ a facet of $f(\mathcal{P})$, $\mathcal{N}_{\mathcal{F}}$ stands for the exterior-pointing normal to $\mathcal{F}$. In particular, $\mathcal{N}_{\mathrm{ind}(\mathcal{V})}$ is the matrix whose columns are formed by the exterior-pointing normals to each facet of $\mathrm{ind}(\mathcal{V})$. A complete exposition on the theory of convex polytopes can be found in [51] and [52].

Given a set $S \in \mathbb{R}^n$ a smooth convex set and $\mathcal{V}$ is an element of its boundary, $\mathcal{N}_{\mathcal{V}}$ stands for the exterior-pointing normal to the supporting hyperplane of S at $\mathcal{V}$.

When considering the scheduling vector $\theta \in \Omega \subseteq \mathbb{R}^{n_\theta}$, for concision and readability, $\theta_{(i)}$ is denoted θ_i directly. Moreover, from (8) to the end of the paper, the dependence of θ on x, u, σ and t is implicit, and θ is generally a shorthand for $\theta(x(t), u(t), \sigma(t), t)$.

3. The General NLSA

The NLSA is a two-step procedure to obtain a T-S model (2) which exactly represents a nonlinear system (1) on a peculiar set. In this section, the two steps of the NLSA procedure are described succinctly, and a nonlinear system is introduced to illustrate the first step of this procedure. This nonlinear system is reused in each section of the paper with variation on the second step of the NLSA.

3.1. NLSA method

Step 1: The first step of the NLSA consists in rewriting (1) as a general LPV system of the following form:

$$\delta x(t) = A(\theta)x(t) + B(\theta)u(t) + \alpha(\theta) \tag{8a}$$

$$y(t) = C(\theta)x(t) + D(\theta)u(t) + \beta(\theta) \tag{8b}$$

with $\theta \in \mathbb{R}^{n_\theta}$ a scheduling vector standing for the nonlinearities and exogenous signals of (1), and A, B, α, C, D, β affine functions of θ. Indeed, θ is chosen such that for all $E \in \{A, B, \alpha, C, D, \beta\}$, $E(\theta)$ can be written as

$$E(\theta) = E_0 + \sum_{i=1}^{n_\theta} \theta_i E_i \tag{9}$$

Remark 3.1. *Several LPV representations are often already possible at this stage, some being more advantageous than others in terms of conservatism reduction or of structural properties (such as controllability and observability). However, this discussion is beyond the scope of this paper, and the interested reader is referred to [35, 36].*

Remark 3.2. *Note that the α and β functions are rarely considered in practice, since they introduce some difficulties in the stability analysis of the model, despite enhancing its representation capabilities.*

Step 2: The second step consists in bounding the values of θ within a set Ω of $\mathbb{R}^{n_\theta}$ with realistic assumptions on $x(t)$, $u(t)$, $\sigma(t)$ and t. From the affine relation between θ and $\{A, B, \alpha, C, D, \beta\}$, the barycentric coordinates of θ within Ω are also the barycentric coordinates of $\{A, B, \alpha, C, D, \beta\}$ within their bounds. Indeed, assuming that Ω is a polytope with vertices $v(\Omega) = \{\mathcal{V}_i\}_{1 \leq i \leq n_\Omega}$ and of barycentric coordinates $(h_1, \ldots, h_{n_\Omega})$, for all $E \in \{A, B, \alpha, C, D, \beta\}$, this "transfer" of barycentric coordinates is easily shown with

the following operations:

$$\begin{aligned} E(\theta) &= E_0 + \sum_{i=1}^{n_\Omega} \theta_i E_i \\ &= E_0 + \sum_{i=1}^{n_\Omega} \left[\sum_{j=1}^{n_\Omega} h_j(\theta) \left(\mathcal{V}_j\right)_{(i)} \right] E_i \\ &= \sum_{j=1}^{n_\Omega} h_j(\theta) \left[E_0 + \sum_{i=1}^{n_\Omega} \left(\mathcal{V}_j\right)_{(i)} E_i \right] \\ E(\theta) &= \sum_{j=1}^{n_\Omega} h_j(\theta) E\left(\mathcal{V}_j\right) \end{aligned} \tag{10}$$

By linearity, this provides a convex-sum representation of (8) for all $x(t)$, $u(t)$, $\sigma(t)$ and t such that $\theta \in \Omega$, which is an exact T-S model representation of (1).

This paper focuses on the second step of the approach. In particular, based on the work of [24] and [27], the next sections provide the barycentric coordinates of θ in Ω respectively when Ω is a polytope (Section 4) or a convex set with a smooth boundary (Section 5). An intuitive measure of the intrinsic conservativeness of the resulting T-S models is given by the size of the subset of Ω that does not contain admissible values of θ [35]. This clearly indicates that some of the previous geometries are better suited for some systems than others depending on the nonlinearities of (1). However, even if this intuitive measure of conservativeness is arguably accurate, some analytical difficulties or simplification can still show up during the practical manipulation of the model and affect the conservativeness of the stability analysis. Rather than providing a single process to obtain the single best NLSA to construct an exact T-S model from a nonlinear system, each section emphasizes the singularity of the presented approach. The authors' goal is to underline the diversity of the possible exact T-S representations obtainable from the NLSA, a topic which is not discussed in the literature yet.

3.2. Application

The T-S models being a convex sum of linear models, it is possible to numerically conduct the stability analysis of these systems through convex optimization techniques, in particular by leveraging results on Quadratic Lyapunov Functions (QLF). Throughout the paper, several T-S representations will be compared in terms of their respective capabilities in the stability analysis of the following second order nonlinear differential equation:

$$\ddot{z} + (1 + \alpha \cos z)\dot{z} + (1 + \beta \sin z)z = 0 \tag{11}$$

which can be re-written as the following system:

$$\begin{bmatrix} \dot{x}_1 \\ \dot{x}_2 \end{bmatrix} = \begin{bmatrix} x_2 \\ -(1 + \beta \sin x_1)x_1 - (1 + \alpha \cos x_1)x_2 \end{bmatrix} \tag{12}$$

with $x_1 = z$ and $x_2 = \dot{z}$. The vector field associated to this differential equation is plotted on Figure 1 for different (α, β) values. For the investigated values, the system displays a typical asymptotically stable behavior. However, the range of (α, β) values for which this property holds is unknown. This will be investigated through several through several exact T-S rewriting of the system, facilitating the numerical stability analysis.

Remark 3.3. *This toy model is arbitrary, and any other system with interdependent nonlinearities could have been chosen to illustrate the generalized NLSA.*

The first step of the NLSA is applied to system (12), which can be re-written as an LPV model (8) by considering a scheduling vector $\theta = \begin{bmatrix} \theta_1 & \theta_2 \end{bmatrix}^\top$ such that

$$\dot{x} = A(\theta)x \tag{13}$$

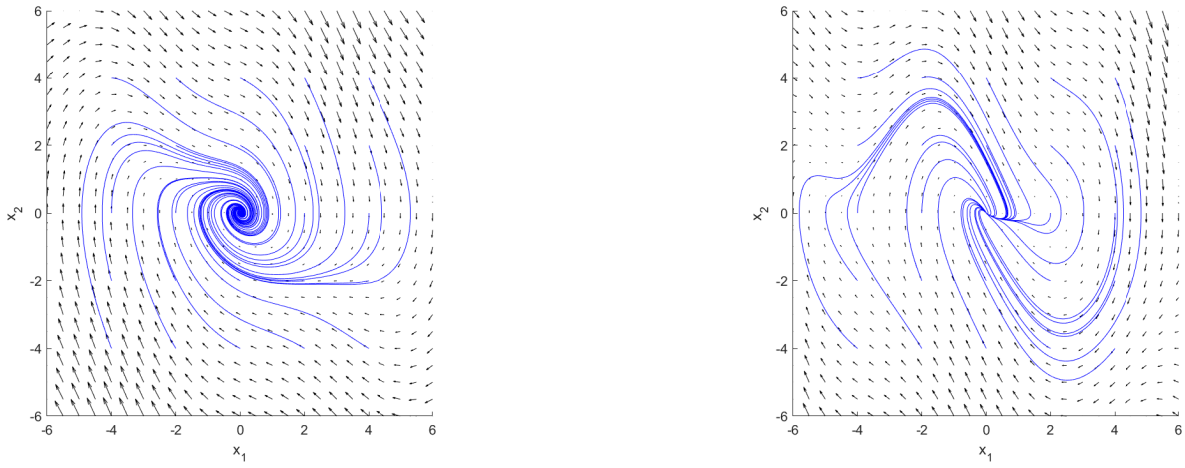

(a) $\alpha = -0.5, \beta = 0.3$ (b) $\alpha = 0.9, \beta = -0.8$

Figure 1: Vector field associated with the differential equation (12) for different (α, β) values, with some trajectories (in blue) converging towards the origin for a set of evenly spread initial conditions.

$$\text{with } A(\theta) = \begin{bmatrix} 0 & 1 \\ -1-\beta\theta_1 & -1-\alpha\theta_2 \end{bmatrix} \text{ and } \begin{cases} \theta_1 = \sin x_1 \\ \theta_2 = \cos x_1 \end{cases} \tag{14}$$

The scheduling parameters (θ_1, θ_2) are interdependent, with $\theta_1^2 + \theta_2^2 = 1$ being always verified. This demonstrates that θ is on the unit circle centered at the origin. Note that these interdependent nonlinearities are also found in real-world dynamical systems, e.g. in the Vertical Take-Off and Landing (VTOL) aircraft model [53, 54], or in the kinematic model of a wheeled mobile robot [55]. Throughout the paper, the unit circle is bounded by a set Ω whose shape varies depending on the considered NLSA. The conservatism of each NLSA is evaluated by comparing the values of α and β for which the resulting T-S representations of (12) are found to be globally exponentially stable. In particular, these results are compared to the following theoretical guarantee, which relies on a QLF.

Lemma 3.1 (Perturbative Approach)**.** *The solutions to* (11) *are globally exponentially stable if*

$$\max(|\alpha|, |\beta|) < 2/(5+\sqrt{5}) \approx 0.27639... \tag{15}$$

Proof. Equation (12) is equivalent to a perturbed system of form

$$\dot{x} = Ax + g(x) \tag{16}$$

$$\text{with } A = \begin{bmatrix} 0 & 1 \\ -1 & -1 \end{bmatrix} \text{ and } g(x) = \begin{bmatrix} 0 \\ -\alpha x_2 \cos x_1 - \beta x_1 \sin x_1 \end{bmatrix} \tag{17}$$

If $P = P^\top \succ 0$ is a positive definite matrix such that $\mathcal{H}(PA) = -I_2$, then $V(x) = x^\top P x$ is a QLF demonstrating that $\dot{x} = Ax$ is globally exponentially stable. It is easy to find such a P.

$$P = \begin{bmatrix} 1.5 & 0.5 \\ 0.5 & 1 \end{bmatrix} \tag{18}$$

Moreover, if $\|g(x)\|_2 \leq \gamma \|x\|_2$ and $\gamma < \frac{1}{2\lambda_{\max}(P)}$, then a result on perturbed systems provides the global exponential stability of (16) as well (see Chapter 9 of [56]). Here, $\gamma = \max(|\alpha|, |\beta|)$ and $\lambda_{\max}(P) = \frac{1}{4}(5+\sqrt{5})$, which concludes the proof. □

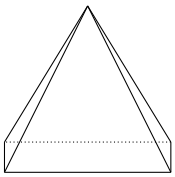

(a) Pyramid of $\mathbb{R}^3$ with a square base

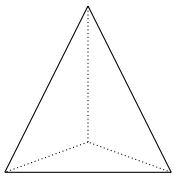

(b) Simplex of $\mathbb{R}^3$

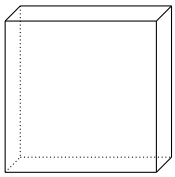

(c) Box of $\mathbb{R}^3$

Figure 2: Illustration of Examples 4.1 and 4.2.

4. The NLSA for Polytopes

This section broadens the well-known NLSA from box-shaped bounding sets to polytopic bounding sets Ω. After defining "simple polytopes" in Definition 4.1, Lemma 4.1 provides the barycentric coordinates of θ inside a simple polytope Ω, and Lemma 4.2 extends these barycentric coordinates to general polytopes. The barycentric coordinates of a box-shaped set are retrieved as a special case of the polytopic barycentric coordinates in Corollary 4.1. Following the procedure of the NLSA, Theorem 4.1 uses these barycentric coordinates as weighting functions in order to obtain a T-S model which exactly represents the nonlinear system (1) for all $\theta \in \Omega$. After discussing the advantages and inconveniences of the NLSA on a polytopic set, a basic result of stability for T-S models is recalled, which is applied to the nonlinear system (11) of Section 3.2 with several geometries for the bounding set Ω.

4.1. NLSA method

Definition 4.1 (Simple Vertex, Simple Polytope [27])**.** *Given a n-dimensional polytope Ω with vertices $v(\Omega) = \{\mathcal{V}_i\}_{1\leq i\leq n_\Omega}$, $\mathcal{V}_i$ is a simple vertex of Ω if $\mathrm{ind}(\mathcal{V}_i)$ has exactly n elements. Otherwise, $\mathcal{V}_i$ is called a non-simple vertex of Ω. The subset of simple vertices (resp. non-simple vertices) of Ω is denoted by $v_s(\Omega) = \{\mathcal{V}_{s(i)}\}_{1\leq i\leq n_s}$ (resp. $v_{\overline{s}}(\Omega)$) with $s : [\![1, n_s]\!] \mapsto [\![1, n_\Omega]\!]$ (resp. $\overline{s}$) an injective function. Ω is called a simple polytope if all of its vertices are simple, i.e. if $v_s(\Omega) = v(\Omega)$.*

Example 4.1. *The four vertices at the base of a pyramid of $\mathbb{R}^3$ with a square base are simple, since they are all contained in exactly three faces of the pyramid. However, its apex is not a simple vertex since it is contained in exactly four faces. Hence, the pyramid is not a simple polytope. This is illustrated in Figure 2a.*

Example 4.2. *All vertices of the n-simplex and of the n-box of $\mathbb{R}^n$ are simple since they are all contained in exactly n facets of these polytopes. Hence, the n-simplex and the n-box are simple polytopes. This is illustrated for $\mathbb{R}^3$ in Figure 2b and 2c.*

Example 4.3. *In general, the 2-dimensional polytopes of $\mathbb{R}^2$ are simple. Indeed, this polytopes are polygons, and every vertex of a polygon is contained in exactly two edges.*

Lemma 4.1 (Barycentric coordinates of a Simple Polytope)**.** *Let $\theta \in \mathbb{R}^{n_\theta}$ be bounded by the simple polytope Ω with vertices $v(\Omega) = \{\mathcal{V}_i\}_{1\leq i\leq n_\Omega}$. For all $i \in [\![1, n_\Omega]\!]$, $w_{\mathcal{V}_i}$ stands for the weight function associated to $\mathcal{V}_i$, with*

$$w_{\mathcal{V}_i}(\theta) = \frac{\left|\det\left(\mathcal{N}_{\mathrm{ind}(\mathcal{V}_i)}\right)\right|}{\prod\limits_{\mathcal{F}\in\mathrm{ind}(\mathcal{V}_i)} \langle \mathcal{N}_\mathcal{F} | \mathcal{V}_i - \theta\rangle} \tag{19}$$

The barycentric coordinates of θ in Ω associated to the vertices $v(\Omega)$ are given by $(h_{\mathcal{V}_i})_{1\leq i\leq n_\Omega}$, a normalization of the previous weights. For all $i \in [\![1, n_\Omega]\!]$, $h_{\mathcal{V}_i}$ is given by

$$h_{\mathcal{V}_i}(\theta) = \frac{w_{\mathcal{V}_i}(\theta)}{\sum\limits_{j=1}^{n_\Omega} w_{\mathcal{V}_j}(\theta)} \tag{20}$$

Proof. For all $n_\Omega \in \mathbb{N}^*$ and $\theta \in \Omega$, the three axioms of barycentric coordinates (3), (4), (6) are verified. The proof that (6) stands can be found in [27], and the two other properties are trivial by construction. □

Corollary 4.1 (Barycentric coordinates of a Box)**.** *Let $\theta \in \mathbb{R}^{n_\theta}$ be bounded by the box-shaped polytope $\Omega = [\underline{\theta}_1, \overline{\theta}_1] \times \cdots \times [\underline{\theta}_{n_\theta}, \overline{\theta}_{n_\theta}]$, i.e. by the convex hull of $\{\mathcal{V}_i\}_{1 \leq i \leq 2^{n_\theta}}$ with for all $i \in [\![1, 2^{n_\theta}]\!]$*

$$\mathcal{V}_i = \mathcal{V}_{\overline{(i-1)_{[n_\theta]} \ldots (i-1)_{[1]}}^{(2)} + 1} \text{ with, for all } k \in [\![1, n_\theta]\!], (\mathcal{V}_i)_{(k)} = \begin{cases} \overline{\theta}_k & \text{if } (i-1)_{[k]} = 1 \\ \underline{\theta}_k & \text{if } (i-1)_{[k]} = 0 \end{cases} \tag{21}$$

For all $i \in [\![1, 2^{n_\theta}]\!]$, let K_i^+ and K_i^- stand for the indices of the digits equal to 1 or 0 resp. in the standard base-2 positional notation of $(i-1)$. Formally:

$$K_i^+ = \left\{k \in [\![1, n_\theta]\!] \ : \ (i-1)_{[k]} = 1\right\} \tag{22a}$$
$$K_i^- = \left\{k \in [\![1, n_\theta]\!] \ : \ (i-1)_{[k]} = 0\right\} \tag{22b}$$

The barycentric coordinates of θ in Ω associated to the vertices $\{\mathcal{V}_i\}_{1 \leq i \leq 2^{n_\theta}}$ are given by $(h_{\mathcal{V}_i})_{1 \leq i \leq 2^{n_\theta}}$ with for all $i \in [\![1, 2^{n_\theta}]\!]$

$$h_{\mathcal{V}_i}(\theta) = \frac{1}{\prod_{k=1}^{n_\theta} (\overline{\theta}_k - \underline{\theta}_k)} \left(\prod_{k \in K_i^-} (\overline{\theta}_k - \theta_k) \right) \left(\prod_{k \in K_i^+} (\theta_k - \underline{\theta}_k) \right) \tag{23}$$

Proof. The barycentric coordinates functions constructed for boxes [24] and simple polytopes [27] are rational functions of the same minimal degree. By unicity of the barycentric coordinates of minimal degree, the two constructions are necessarily equal to each other when a box is considered [57]. To verify this claim, the barycentric coordinates of a box are retrieved below from the formula of the barycentric coordinates of a simple polytope. Taking $n_\Omega = 2^{n_\theta}$, $\Omega = [\underline{\theta}_1, \overline{\theta}_1] \times \cdots \times [\underline{\theta}_{n_\theta}, \overline{\theta}_{n_\theta}]$, the facets of the polytope Ω are given by $f(\Omega) = \left\{\mathcal{F}_k^+, \mathcal{F}_k^-\right\}_{1 \leq k \leq n_\theta}$, with for all $k \in [\![1, n_\theta]\!]$

$$\mathcal{F}_k^+ = \text{Hull}\left\{\mathcal{V}_i : i \in [\![1, 2^{n_\theta}]\!] \,|\, k \in K_i^+\right\} \tag{24a}$$
$$\mathcal{F}_k^- = \text{Hull}\left\{\mathcal{V}_i : i \in [\![1, 2^{n_\theta}]\!] \,|\, k \in K_i^-\right\} \tag{24b}$$

By denoting $(e_1, \ldots, e_{n_\theta})$ the standard basis of $\mathbb{R}^{n_\theta}$, it is clear that the normals to the facets of Ω are simply given by $\mathcal{N}_{\mathcal{F}_k^+} = e_k$ and $\mathcal{N}_{\mathcal{F}_k^-} = -e_k$. Moreover, for all $i \in [\![1, 2^{n_\theta}]\!]$

$$\text{ind}(\mathcal{V}_i) = \left\{\mathcal{F}_k^+ : k \in [\![1, n_\theta]\!] \,|\, k \in K_i^+\right\} \cup \left\{\mathcal{F}_k^- : k \in [\![1, n_\theta]\!] \,|\, k \in K_i^-\right\} \tag{25}$$

hence $\left|\det\left(\mathcal{N}_{\text{ind}(\mathcal{V}_i)}\right)\right| = 1$, and

$$\begin{aligned} \prod_{\mathcal{F} \in \text{ind}(\mathcal{V}_i)} \langle \mathcal{N}_\mathcal{F} | \mathcal{V}_i - \theta \rangle &= \left(\prod_{k \in K_i^+} \langle \mathcal{N}_{\mathcal{F}_k^+} | \mathcal{V}_i - \theta \rangle \right) \left(\prod_{k \in K_i^-} \langle \mathcal{N}_{\mathcal{F}_k^-} | \mathcal{V}_i - \theta \rangle \right) \\ &= \left(\prod_{k \in K_i^+} (\overline{\theta}_k - \theta_k) \right) \left(\prod_{k \in K_i^-} (\theta_k - \underline{\theta}_k) \right) \end{aligned} \tag{26}$$

which yields

$$\sum_{i=1}^{2^{n_\theta}} w_{\mathcal{V}_i}(\theta) = \sum_{i=1}^{2^{n_\theta}} \frac{1}{\left(\prod_{k \in K_i^+} (\overline{\theta}_k - \theta_k)\right) \left(\prod_{k \in K_i^-} (\theta_k - \underline{\theta}_k)\right)} \tag{27}$$

noticing that K_i^+ and K_i^- form a partition of $[\![1, n_\theta]\!]$ for all $i \in [\![1, 2^{n_\theta}]\!]$, multiplying the numerator and denominator of each term in the sum by $\left(\prod_{k\in K_i^-}(\overline{\theta}_k - \theta_k)\right)\left(\prod_{k\in K_i^+}(\theta_k - \underline{\theta}_k)\right)$ provides

$$\sum_{i=1}^{2^{n_\theta}} w_{\mathcal{V}_i}(\theta) = \frac{1}{\prod_{k=1}^{n_\theta}(\overline{\theta}_k - \theta_k)(\theta_k - \underline{\theta}_k)} \sum_{i=1}^{2^{n_\theta}} \left(\prod_{k\in K_i^-}(\overline{\theta}_k - \theta_k)\right)\left(\prod_{k\in K_i^+}(\theta_k - \underline{\theta}_k)\right) \tag{28}$$

finally, the fact that $K^+_{2^{n_\theta}+1-i} = K_i^-$ (resp. $K^-_{2^{n_\theta}+1-i} = K_i^+$) makes it possible to re-order the terms of the sum, and obtain

$$\begin{aligned}\sum_{i=1}^{2^{n_\theta}} w_{\mathcal{V}_i}(\theta) &= \frac{1}{\prod_{k=1}^{n_\theta}(\overline{\theta}_k - \theta_k)(\theta_k - \underline{\theta}_k)} \sum_{i=1}^{2^{n_\theta}} \left(\prod_{k\in K_i^+}(\overline{\theta}_k - \theta_k)\right)\left(\prod_{k\in K_i^-}(\theta_k - \underline{\theta}_k)\right) \\ &= \frac{1}{\prod_{k=1}^{n_\theta}(\overline{\theta}_k - \theta_k)(\theta_k - \underline{\theta}_k)} \left(\sum_{i=1}^{2^{n_\theta}} \frac{1}{w_{\mathcal{V}_i}(\theta)}\right)\end{aligned} \tag{29}$$

By a succession of factorization, one has

$$\begin{aligned}
&\sum_{i=1}^{2^{n_\theta}} \frac{1}{w_{\mathcal{V}_i}(\theta)} = \sum_{i=1}^{2^{n_\theta}} \left(\prod_{k\in K_i^-}(\overline{\theta}_k - \theta_k)\right)\left(\prod_{k\in K_i^+}(\theta_k - \underline{\theta}_k)\right) \\
&= \left[(\overline{\theta}_{n_\theta} - \theta_{n_\theta}) + (\theta_{n_\theta} - \underline{\theta}_{n_\theta})\right] \sum_{i=1}^{2^{n_\theta-1}} \left(\prod_{k\in K_i^-\setminus\{n_\theta\}}(\overline{\theta}_k - \theta_k)\right)\left(\prod_{k\in K_i^+\setminus\{n_\theta\}}(\theta_k - \underline{\theta}_k)\right) \\
&= \left(\overline{\theta}_{n_\theta} - \underline{\theta}_{n_\theta}\right) \sum_{i=1}^{2^{n_\theta-1}} \left(\prod_{k\in K_i^-\setminus\{n_\theta\}}(\overline{\theta}_k - \theta_k)\right)\left(\prod_{k\in K_i^+\setminus\{n_\theta\}}(\theta_k - \underline{\theta}_k)\right) \\
&= \left(\overline{\theta}_{n_\theta} - \underline{\theta}_{n_\theta}\right)\left(\overline{\theta}_{n_\theta-1} - \underline{\theta}_{n_\theta-1}\right) \sum_{i=1}^{2^{n_\theta-2}} \left(\prod_{k\in K_i^-\setminus\{n_\theta, n_\theta-1\}}(\overline{\theta}_k - \theta_k)\right)\left(\prod_{k\in K_i^+\setminus\{n_\theta, n_\theta-1\}}(\theta_k - \underline{\theta}_k)\right) \\
&= \dots \\
&= \left[\prod_{k=3}^{n_\theta}\left(\overline{\theta}_k - \underline{\theta}_k\right)\right]\left[(\overline{\theta}_2 - \theta_2)\left((\overline{\theta}_1 - \theta_1) + (\theta_1 - \underline{\theta}_1)\right) + (\theta_2 - \underline{\theta}_2)\left((\overline{\theta}_1 - \theta_1) + (\theta_1 - \underline{\theta}_1)\right)\right] \\
&= \left[(\overline{\theta}_2 - \theta_2) + (\theta_2 - \underline{\theta}_2)\right]\left[\prod_{k=3}^{n_\theta}\left(\overline{\theta}_k - \underline{\theta}_k\right)\right]\left((\overline{\theta}_1 - \theta_1) + (\theta_1 - \underline{\theta}_1)\right) \\
&= \left[\prod_{k=2}^{n_\theta}\left(\overline{\theta}_k - \underline{\theta}_k\right)\right]\left((\overline{\theta}_1 - \theta_1) + (\theta_1 - \underline{\theta}_1)\right) \\
&= \prod_{k=1}^{n_\theta}\left(\overline{\theta}_k - \underline{\theta}_k\right)
\end{aligned} \tag{30}$$

Injecting the expression of $\sum_{j=1}^{2^{n_\theta}} w_{\mathcal{V}_j}(\theta)$ and $w_{\mathcal{V}_i}(\theta)$ in $h_{\mathcal{V}_i}(\theta)$ provides

$$\begin{aligned} h_{\mathcal{V}_i}(\theta) &= \frac{w_{\mathcal{V}_i}(\theta)}{\sum_{j=1}^{n_\Omega} w_{\mathcal{V}_j}(\theta)} \\ &= \frac{1}{\prod_{k=1}^{n_\theta}(\overline{\theta}_k - \underline{\theta}_k)} \cdot \left(\prod_{k=1}^{n_\theta} (\overline{\theta}_k - \theta_k)(\theta_k - \underline{\theta}_k) \right) w_{\mathcal{V}_i}(\theta) \\ h_{\mathcal{V}_i}(\theta) &= \frac{1}{\prod_{k=1}^{n_\theta}(\overline{\theta}_k - \underline{\theta}_k)} \cdot \frac{\prod_{k=1}^{n_\theta}(\overline{\theta}_k - \theta_k)(\theta_k - \underline{\theta}_k)}{\left(\prod_{k\in K_i^+}(\overline{\theta}_k - \theta_k)\right)\left(\prod_{k\in K_i^-}(\theta_k - \underline{\theta}_k)\right)} \end{aligned} \tag{31}$$

and finally, leveraging again the partition of $[\![1, n_\theta]\!]$ by K_i^+ and K_i^- gives

$$\begin{aligned} h_{\mathcal{V}_i}(\theta) &= \frac{1}{\prod_{k=1}^{n_\theta}(\overline{\theta}_k - \underline{\theta}_k)} \cdot \frac{\prod_{k=1}^{n_\theta}(\overline{\theta}_k - \theta_k)(\theta_k - \underline{\theta}_k)}{\left(\prod_{k\in K_i^+}(\overline{\theta}_k - \theta_k)\right)\left(\prod_{k\in K_i^-}(\theta_k - \underline{\theta}_k)\right)} \\ &= \frac{1}{\prod_{k=1}^{n_\theta}(\overline{\theta}_k - \underline{\theta}_k)} \left(\prod_{k\in K_i^-} (\overline{\theta}_k - \theta_k) \right) \left(\prod_{k\in K_i^+} (\theta_k - \underline{\theta}_k) \right) \end{aligned} \tag{32}$$

which is the expression (23). □

The previous barycentric coordinates can be extended to all kinds of polytopes with a perturbation trick where the non-simple vertices of the polytopes are decomposed into several simple vertices. The idea of this trick is given succinctly in the Lemma 4.2, and the rigorous proof of the invariance of the weight functions under the infinitesimal decomposition of non-simple vertices is found in [58].

Lemma 4.2 (Barycentric coordinates of a Polytope)**.** *Let $\theta \in \mathbb{R}^{n_\theta}$ be bounded by the polytope Ω with vertices $v(\Omega) = \{\mathcal{V}_i\}_{1\leq i\leq n_\Omega}$. Each non-simple vertex $\mathcal{V}_{\overline{s}(i)} \in v_{\overline{s}}(\Omega)$ is infinitesimally disturbed into m_i distinct vertices $w_i = \{\mathcal{W}_j\}_{1\leq j\leq m_i}$ such that the polytope Ω_s given by the convex hull of $v_s(\Omega) \cup (\bigcup_{i=1}^{n_{\overline{s}}} w_i)$ is simple. For all $\mathcal{V}_{\overline{s}(i)} \in v_{\overline{s}}(\Omega)$, the weight function of $\mathcal{V}_{\overline{s}(i)}$ in Ω is given by summing the weight functions of the simple vertices w_i in Ω_s. Moreover, for all $\mathcal{V}_{s(i)} \in v_s(\Omega)$, the weight function of $\mathcal{V}_{s(i)}$ stays unchanged between Ω and Ω_s. Formally:*

$$w^{\Omega}_{\mathcal{V}_{s(i)}}(\theta) = w^{\Omega_s}_{\mathcal{V}_{s(i)}}(\theta) \tag{33a}$$

$$w^{\Omega}_{\mathcal{V}_{\overline{s}(i)}}(\theta) = \sum_{j=1}^{m_i} w^{\Omega_s}_{\mathcal{W}_j}(\theta) \tag{33b}$$

The weight functions for the simple vertices Ω_s are defined in Lemma 4.1. The barycentric coordinates of θ in Ω associated to the vertices $v(\Omega)$ are finally given by normalizing the previous weights, as in Lemma 4.1.

Keeping the notations of Lemmas 4.1 and 4.2, the following generalization of the NLSA on a polytope can be stated.

Theorem 4.1 (NLSA on a Polytope)**.** *The T-S model (34) is an exact representation of the nonlinear system (1) for all $x(t)$, $u(t)$, $\sigma(t)$ and t such that $\theta \in \Omega$.*

$$\delta x(t) = \sum_{i=1}^{n_\Omega} h_{\mathcal{V}_i}(\theta) \left[A(\mathcal{V}_i)x(t) + B(\mathcal{V}_i)u(t) + \alpha(\mathcal{V}_i) \right] \tag{34a}$$

$$y(t) = \sum_{i=1}^{n_\Omega} h_{\mathcal{V}_i}(\theta) \left[C(\mathcal{V}_i)x(t) + D(\mathcal{V}_i)u(t) + \beta(\mathcal{V}_i) \right] \tag{34b}$$

The intrinsic conservatism of the usual NLSA on a box-shaped bounding set is generally fair if the initial nonlinear system (1) has independent and narrowly bounded scheduling parameters θ_i. Moreover, the barycentric coordinates $(h_{\mathcal{V}_i})_{1\leq i\leq 2^{n_\theta}}$ are very easy to construct and are polynomial in the scheduling parameters (see Corollary 4.1), which allows for some conservatism reduction in the stability analysis [59, 43]. However, the resulting T-S model needs a number of vertices which is exponentially growing ($n_\Omega = 2^{n_\theta}$) in the number of scheduling parameters, and it generally ceases to be the best representation as long as some of the scheduling parameters are not fully decoupled and show some interdependencies.

In comparison, the extension of the NLSA to polytopic bounding sets has a lot of advantages: the number of vertices needed is flexible, and can be chosen to be linearly growing ($n_\Omega = n_\theta + 1$) in the number of scheduling parameters by bounding θ within a simplex. It also appears to be extremely useful in order to minimize the intrinsic conservatism of the T-S model when the scheduling parameters are not fully decoupled and show some interdependencies. Indeed, moving away from the box-shaped framework, it is now possible to get rid of some useless vertices of the model earlier than in other works [48], or to move some vertices around, which can easily reduce the size of the subset of Ω that does not contain admissible values of θ, hence reducing the intrinsic conservatism of the T-S model. Finally, the barycentric coordinates $(h_{\mathcal{V}_i})_{1\leq i\leq n_\Omega}$ are rational functions of the scheduling parameters, which could possibly be leveraged for some conservatism reduction, by taking inspiration from the results found in [59, 43].

However, this extension has a few weaknesses: in high dimensions, the construction of such models can be laborious, the bounding polytope being hard to determine, and the non-simple vertices challenging to handle. Moreover, the computation of the weight functions behind the barycentric coordinates of the model also involves some divisions by zero, which do not cause any theoretical problem (by a simple argument of continuity), but which have to be taken care of numerically, for example in PDC schemes. Note that this generalization of the NLSA for T-S models was already mentioned, solely for simple polytopes, in Section 2.1.2 of [25].

4.2. Bounding methodology

Contrary to the usual NLSA on a box-shaped bounding set, bounding interdependent nonlinearities within a small polytope Ω is a much harder problem in high dimensions. However, this problem is not new, and several techniques to find minimal bounding polytopes are already known in the LPV literature (see [49] for a review) and can be leveraged to this end. Generally speaking, the techniques consist in the two following steps:

- sample the scheduling vector θ for x, u, σ and t in a range of interest, possibly with random noise to increase robustness;
- compute the convex hull of all the obtained points using a dedicated algorithm (such as the well-known "quick hull" [60]).

The resulting convex hull provides a vertex-representation (V-representation) of the bounding polytope. However, in addition to the usual LPV methodology, the polytopic NLSA provides an expression for the activation functions $(h_{\mathcal{V}_i})_{1\leq i\leq n_\Omega}$. For this expression to be properly determined algorithmically, one must:

- disturb the non-simple vertices of the bounding polytope until the polytope becomes simple [61];
- compute normals to the facets, which is equivalent to computing the half-space-representation (H-representation) of the polytope [52, 51].

Thankfully, all these computationally heavy steps just need to be perfomed once. After the V- and H-representations of the bounding polytope Ω are obtained, the expression of $h_{\mathcal{V}_i}(\theta)$ can be evaluated in real time, for example to compute PDC control laws.

4.3. Stability Analysis

The previously presented generalized NLSA is now used for stability analysis. No new stabilty results are provided here, but the objective is to illustrate the conservatism reduction brought by the generalized NLSA compared to the usual box approach. Given the continuous-time and input-free T-S model (35),

$$\dot{x}(t) = \sum_{i=1}^{n_\Omega} h_i(\theta) A_i x(t) \tag{35}$$

the most widespread approach to stability analysis of T-S models relies on a direct Lyapunov method. In particular, introducing a QLF is the simplest way to obtain a system of LMI conditions, that, if satisfied, demonstrates the exponential stability of the T-S model. Given the QLF (36)

$$V(x) = x^\top P x \tag{36}$$

with $P = P^\top \succ 0$, these LMI conditions are stated as follows:

Theorem 4.2 (Quadratic Stability [62])**.** *The T-S model (35) is globally exponentially stable if there exists $P = P^\top \in \mathbb{R}^{n_x \times n_x}$ such that the LMI conditions (37) are satisfied.*

$$P \succ 0 \tag{37a}$$

$$\forall j \in J,\ \mathcal{H}(PA_j) \prec 0 \tag{37b}$$

Where J is a subset of $[\![1, n_\Omega]\!]$ such that for all $i \in [\![1, n_\Omega]\!]$, $A_i \in \mathrm{Hull}\{A_j : j \in J\}$.

Proof. It is assumed that the LMIs (37) hold. For all $j \in J$, the matrices $\mathcal{H}(PA_j)$ and $-P$ are real, symmetric and negative definite, meaning all their eigenvalues are strictly negative. Hence, there exists $\varepsilon \in \mathbb{R}_{>0}$ such that for all $j \in J$, $\lambda_{\max}\left[\mathcal{H}(PA_j)\right] < 2\varepsilon\lambda_{\min}(-P)$, providing $\lambda_{\max}\left[\mathcal{H}(PA_j) + 2\varepsilon P\right] < 0$ and finally $\mathcal{H}(PA_j) \prec -2\varepsilon P$ by a simple application of Weyl's inequalities on Hermitian matrices [63]. By convexity, for all $X \in \mathrm{Hull}\{A_j : j \in J\}$, $\mathcal{H}\left(PX\right) \prec -2\varepsilon P$, that is to say, for all $\theta \in \Omega$

$$\mathcal{H}\left(P \sum_{i=1}^{n_\theta} h_i(\theta) A_i\right) \prec -2\varepsilon P \tag{38}$$

Introducing (36) as a QLF, the previous equation provides $\dot{V}(x(t)) \leq -2\varepsilon V(x(t))$. Grönwall's inequality then yields

$$V(x(t)) \leq e^{-2\varepsilon(t-t_0)} V(x(t_0)) \tag{39}$$

Moreover, since $\lambda_{\min}(P) I_{n_x} \preceq P \preceq \lambda_{\max}(P) I_{n_x}$, it is easy to find

$$\|x(t)\| \leq \sqrt{\frac{\lambda_{\max}(P)}{\lambda_{\min}(P)}} e^{-\varepsilon(t-t_0)} \|x(t_0)\| \tag{40}$$

which demonstrates that the T-S model (35) is globally exponentially stable. □

Remark 4.1. *For T-S models obtained through the NLSA when Ω is a polytopic set, by construction $J = [\![1, n_\Omega]\!]$. This means that not a single local model obtained through the polytopic NLSA is useless in the LMI-based stability analysis described above.*

This result is rudimentary and introduces some conservativeness in the stability analysis. Less conservative approaches usually involve a nonquadratic Lyapunov function and lead to an LMI optimization problem of higher dimension. The most commonly used nonquadratic Lyapunov functions are the multiquadratic Lyapunov functions, also known as the polyquadratic Lyapunov functions or the fuzzy Lyapunov functions [39, 46], and the piecewise quadratic Lyapunov functions [37, 38, 45]. This paper only considers QLF in order to compare different T-S models on an equal footing. It is expected that using more sophisticated Lyapunov functions improves the results obtained with the different models without changing which models perform better than the others. This is succinctly illustrated by Remark 4.2 and Figure 9, where the piecewise quadratic Lyapunov function of [38] is used in the stability analysis.

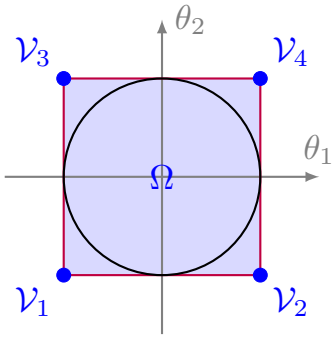

Figure 3: The box-shaped set Ω is bounding the scheduling vector θ of (13)

4.4. Application

The previous results are applied to the nonlinear system (11) of Section 3.2 by using three different bounding sets Ω for the scheduling vector θ of the LPV model (13). The first one is chosen to be a box (the usual approach), the second one is chosen to be an hexagon, and the last one is chosen to be an octagon. As expected, it is shown that the stability results obtained using the octagonal bounding set are less conservative than those obtained using the hexagonal bounding set, which are themselves arguably less conservative than those obtained using the box-shaped bounding set. Note that the hexagon is not strictly included in the square box, even if its area is lower.

4.4.1. Box-shaped bounding set

Considering the LPV model (13), the box $\Omega = [-1, 1]^2$ is chosen to be the bounding set of θ. As illustrated by Figure 3, Ω has four vertices:

$$\mathcal{V}_1 = \begin{bmatrix} -1 & -1 \end{bmatrix}^\top \tag{41a}$$
$$\mathcal{V}_2 = \begin{bmatrix} 1 & -1 \end{bmatrix}^\top \tag{41b}$$
$$\mathcal{V}_3 = \begin{bmatrix} -1 & 1 \end{bmatrix}^\top \tag{41c}$$
$$\mathcal{V}_4 = \begin{bmatrix} 1 & 1 \end{bmatrix}^\top \tag{41d}$$

The barycentric coordinates of θ are given by Corollary 4.1:

$$h_{\mathcal{V}_1}(\theta) = \frac{1}{4}(1-\theta_1)(1-\theta_2) \tag{42a}$$
$$h_{\mathcal{V}_2}(\theta) = \frac{1}{4}(1+\theta_1)(1-\theta_2) \tag{42b}$$
$$h_{\mathcal{V}_3}(\theta) = \frac{1}{4}(1-\theta_1)(1+\theta_2) \tag{42c}$$
$$h_{\mathcal{V}_4}(\theta) = \frac{1}{4}(1+\theta_1)(1+\theta_2) \tag{42d}$$

Finally, the NLSA on the box Ω is completed and the system (12) is exactly represented by the following T-S model:

$$\dot{x}(t) = \sum_{i=1}^{4} h_{\mathcal{V}_i}(\theta) A(\mathcal{V}_i) x(t) \tag{43}$$

The stability analysis of the T-S model (43) is performed using Theorem 4.2 at several $(\alpha, \beta) \in \mathbb{R}^2$ values. The (α, β)-region for which the system (43) is found to be stable is plotted on Figure 4, where it is compared to the (α, β)-region obtained with the perturbative approach of Section 3.2. The (α, β)-region of stability is visibly larger with Theorem 4.2 than with the perturbative approach, but contrary to the perturbative approach, the region is only a discrete subset of the (α, β)-plane.

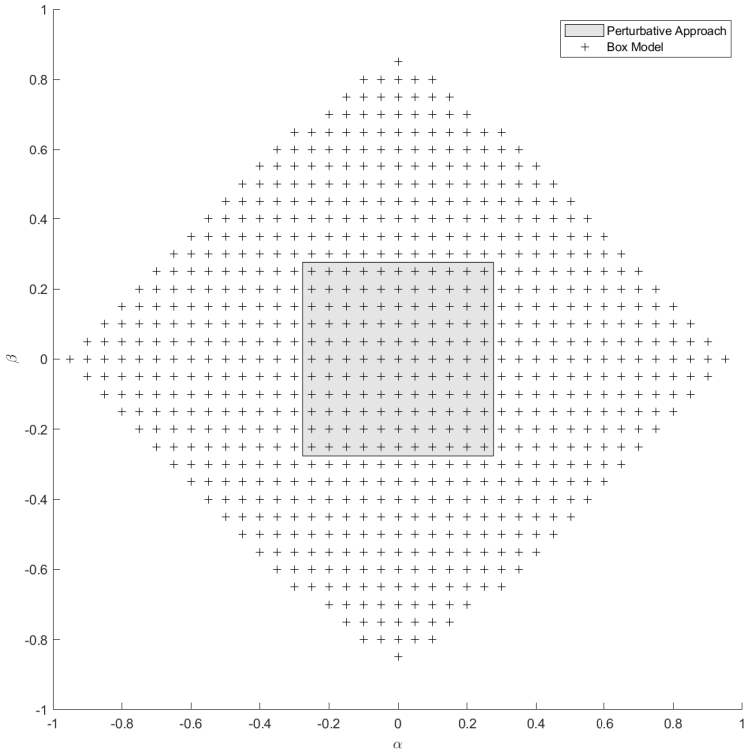

Figure 4: Stability (α, β)-regions of (11) using Theorem 4.2 on the T-S model (43) (box model), and using the perturbative approach of Section 3.2

4.4.2. Hexagonal bounding set

Similarly, the regular hexagon $\Omega = \text{Hull}\{\mathcal{V}_1, \ldots, \mathcal{V}_6\}$ is chosen to be the bounding set of θ. As illustrated by Figure 5, Ω has six vertices:

$$\mathcal{V}_1 = \begin{bmatrix} \frac{2}{\sqrt{3}} & 0 \end{bmatrix}^\top \tag{44a}$$
$$\mathcal{V}_2 = \begin{bmatrix} \frac{1}{\sqrt{3}} & 1 \end{bmatrix}^\top \tag{44b}$$
$$\mathcal{V}_3 = \begin{bmatrix} -\frac{1}{\sqrt{3}} & 1 \end{bmatrix}^\top \tag{44c}$$
$$\mathcal{V}_4 = \begin{bmatrix} -\frac{2}{\sqrt{3}} & 0 \end{bmatrix}^\top \tag{44d}$$
$$\mathcal{V}_5 = \begin{bmatrix} -\frac{1}{\sqrt{3}} & -1 \end{bmatrix}^\top \tag{44e}$$
$$\mathcal{V}_6 = \begin{bmatrix} \frac{1}{\sqrt{3}} & -1 \end{bmatrix}^\top \tag{44f}$$

This polytope has six facets $f(\Omega) = \{\mathcal{F}_1, \ldots, \mathcal{F}_6\}$, with for all $i \in [\![1, 5]\!]$, $\mathcal{F}_i = \text{Hull}\{\mathcal{V}_i, \mathcal{V}_{i+1}\}$ and $\mathcal{F}_6 = \text{Hull}\{\mathcal{V}_1, \mathcal{V}_6\}$. The normals to these facets are given below.

$$\mathcal{N}_{\mathcal{F}_1} = \begin{bmatrix} \frac{\sqrt{3}}{2} & \frac{1}{2} \end{bmatrix}^\top \tag{45a}$$
$$\mathcal{N}_{\mathcal{F}_2} = \begin{bmatrix} 0 & 1 \end{bmatrix}^\top \tag{45b}$$
$$\mathcal{N}_{\mathcal{F}_3} = \begin{bmatrix} -\frac{\sqrt{3}}{2} & \frac{1}{2} \end{bmatrix}^\top \tag{45c}$$
$$\mathcal{N}_{\mathcal{F}_4} = \begin{bmatrix} -\frac{\sqrt{3}}{2} & -\frac{1}{2} \end{bmatrix}^\top \tag{45d}$$
$$\mathcal{N}_{\mathcal{F}_5} = \begin{bmatrix} 0 & -1 \end{bmatrix}^\top \tag{45e}$$
$$\mathcal{N}_{\mathcal{F}_6} = \begin{bmatrix} \frac{\sqrt{3}}{2} & -\frac{1}{2} \end{bmatrix}^\top \tag{45f}$$

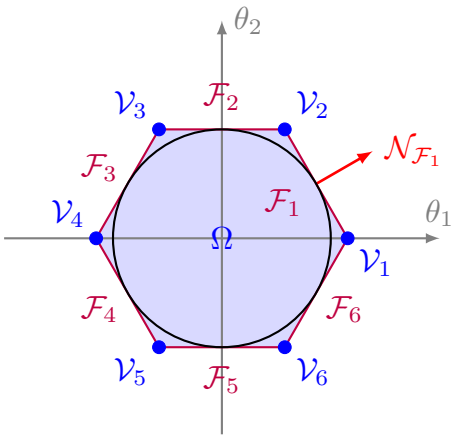

Figure 5: The hexagonal set Ω is bounding the scheduling vector θ of (13)

The polytope being 2-dimensional, it is a simple polytope, moreover $\mathrm{ind}(\mathcal{V}_1) = \{\mathcal{F}_6, \mathcal{F}_1\}$ and for all $i \in [\![2, 6]\!]$, $\mathrm{ind}(\mathcal{V}_i) = \{\mathcal{F}_{i-1}, \mathcal{F}_i\}$. The weight functions are computed using Lemma 4.1:

$$w_{\mathcal{V}_1}(\theta) = \frac{2\sqrt{3}}{3\theta_1^2 - 4\sqrt{3}\theta_1 - \theta_2^2 + 4} \tag{46a}$$

$$w_{\mathcal{V}_2}(\theta) = \frac{\sqrt{3}}{(\theta_2 - 1)(\sqrt{3}\theta_1 + \theta_2 - 2)} \tag{46b}$$

$$w_{\mathcal{V}_3}(\theta) = \frac{\sqrt{3}}{(\theta_2 - 1)(-\sqrt{3}\theta_1 + \theta_2 - 2)} \tag{46c}$$

$$w_{\mathcal{V}_4}(\theta) = \frac{2\sqrt{3}}{3\theta_1^2 + 4\sqrt{3}\theta_1 - \theta_2^2 + 4} \tag{46d}$$

$$w_{\mathcal{V}_5}(\theta) = \frac{\sqrt{3}}{(\theta_2 + 1)(\sqrt{3}\theta_1 + \theta_2 + 2)} \tag{46e}$$

$$w_{\mathcal{V}_6}(\theta) = \frac{\sqrt{3}}{(\theta_2 + 1)(-\sqrt{3}\theta_1 + \theta_2 + 2)} \tag{46f}$$

which provides the barycentric coordinates of θ within the hexagon Ω:

$$h_{\mathcal{V}_1}(\theta) = \frac{(\theta_2^2 - 1)(3\theta_1^2 + 4\sqrt{3}\theta_1 - \theta_2^2 + 4)}{6(\theta_1^2 + \theta_2^2 - 4)} \tag{47a}$$

$$h_{\mathcal{V}_2}(\theta) = \frac{(\theta_2 + 1)(-\sqrt{3}\theta_1 + \theta_2 - 2)(-3\theta_1^2 + \theta_2^2 + 4\theta_2 + 4)}{12(\theta_1^2 + \theta_2^2 - 4)} \tag{47b}$$

$$h_{\mathcal{V}_3}(\theta) = \frac{(\theta_2 + 1)(\sqrt{3}\theta_1 + \theta_2 - 2)(-3\theta_1^2 + \theta_2^2 + 4\theta_2 + 4)}{12(\theta_1^2 + \theta_2^2 - 4)} \tag{47c}$$

$$h_{\mathcal{V}_4}(\theta) = \frac{(\theta_2^2 - 1)(3\theta_1^2 - 4\sqrt{3}\theta_1 - \theta_2^2 + 4)}{6(\theta_1^2 + \theta_2^2 - 4)} \tag{47d}$$

$$h_{\mathcal{V}_5}(\theta) = \frac{(\theta_2 - 1)(\sqrt{3}\theta_1 - \theta_2 - 2)(3\theta_1^2 - \theta_2^2 + 4\theta_2 - 4)}{12(\theta_1^2 + \theta_2^2 - 4)} \tag{47e}$$

$$h_{\mathcal{V}_6}(\theta) = \frac{(\theta_2 - 1)(-\sqrt{3}\theta_1 - \theta_2 - 2)(3\theta_1^2 - \theta_2^2 + 4\theta_2 - 4)}{12(\theta_1^2 + \theta_2^2 - 4)} \tag{47f}$$

Finally, the NLSA on the polytope Ω is completed and the system (12) is exactly represented by the following T-S model:

$$\dot{x}(t) = \sum_{i=1}^{6} h_{\mathcal{V}_i}(\theta) A(\mathcal{V}_i) x(t) \tag{48}$$

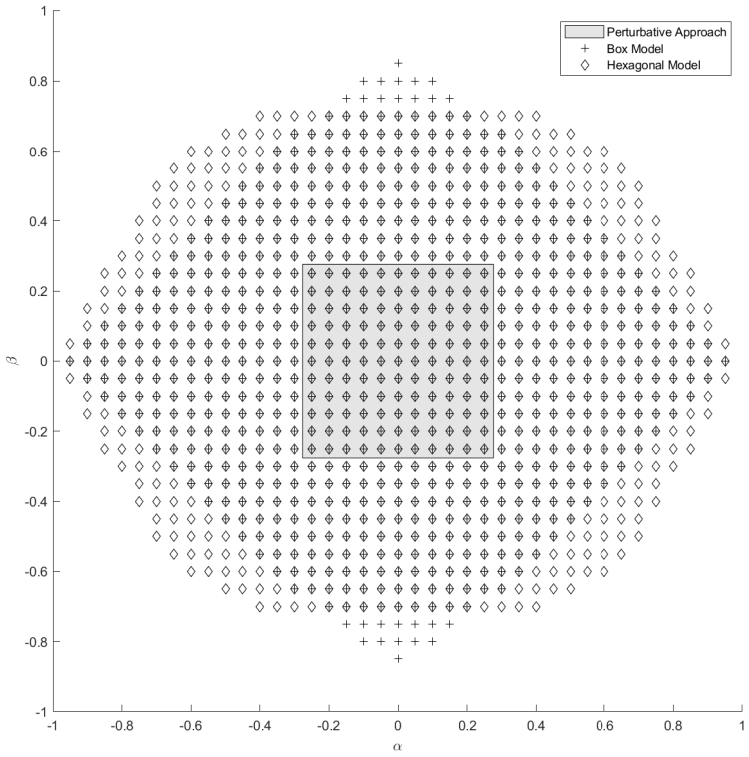

Figure 6: Stability (α, β)-regions of (11) using Theorem 4.2 on the T-S models (48) (hexagonal model), (43) (box model), and using the perturbative approach of Section 3.2

The stability analysis of the T-S model (48) is performed using Theorem 4.2 at several $(\alpha, \beta) \in \mathbb{R}^2$ values. The (α, β)-region for which the system (48) (hexagonal model) is found to be stable is plotted on Figure 6, where it is compared to the (α, β)-region obtained with the T-S model (43) (box model), and with the perturbative approach of Section 3.2. The (α, β)-region of stability is visibly larger by using Theorem 4.2 on the T-S model (48) (hexagonal model) than on the T-S model (43) (box model): indeed, the hexagonal bounding set is sharper than the box-shaped bounding set, which relaxes the conservatism of the stability analysis.

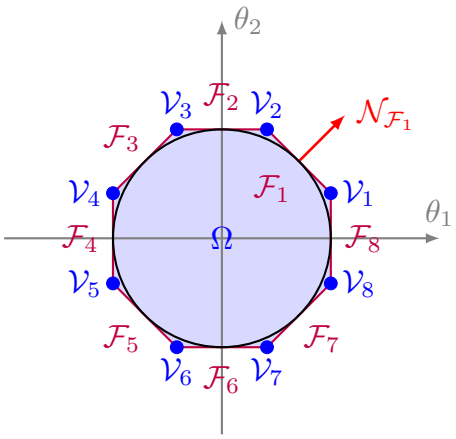

Figure 7: The octagonal set Ω is bounding the scheduling vector θ of (13)

4.4.3. Octagonal bounding set

Finally, the regular octagon $\Omega = \text{Hull}\,\{\mathcal{V}_1, \dots, \mathcal{V}_8\}$ is chosen to be the bounding set of θ. As illustrated by Figure 7, Ω has eight vertices:

$$\mathcal{V}_1 = [\ 1 \quad \sqrt{2}-1\ ]^\top \tag{49a}$$
$$\mathcal{V}_2 = [\ \sqrt{2}-1 \quad 1\ ]^\top \tag{49b}$$
$$\mathcal{V}_3 = [\ -\sqrt{2}+1 \quad 1\ ]^\top \tag{49c}$$
$$\mathcal{V}_4 = [\ -1 \quad \sqrt{2}-1\ ]^\top \tag{49d}$$
$$\mathcal{V}_5 = [\ -1 \quad -\sqrt{2}+1\ ]^\top \tag{49e}$$
$$\mathcal{V}_6 = [\ -\sqrt{2}+1 \quad -1\ ]^\top \tag{49f}$$
$$\mathcal{V}_7 = [\ \sqrt{2}-1 \quad -1\ ]^\top \tag{49g}$$
$$\mathcal{V}_8 = [\ 1 \quad -\sqrt{2}+1\ ]^\top \tag{49h}$$

This polytope has eight facets $f(\Omega) = \{\mathcal{F}_1, \dots, \mathcal{F}_8\}$, with for all $i \in [\![1, 7]\!]$, $\mathcal{F}_i = \text{Hull}\{\mathcal{V}_i, \mathcal{V}_{i+1}\}$ and $\mathcal{F}_8 = \text{Hull}\{\mathcal{V}_1, \mathcal{V}_8\}$. The normals to these facets are given below.

$$\mathcal{N}_{\mathcal{F}_1} = [\ \tfrac{1}{\sqrt{2}} \quad \tfrac{1}{\sqrt{2}}\ ]^\top \tag{50a}$$
$$\mathcal{N}_{\mathcal{F}_2} = [\ 0 \quad 1\ ]^\top \tag{50b}$$
$$\mathcal{N}_{\mathcal{F}_3} = [\ -\tfrac{1}{\sqrt{2}} \quad \tfrac{1}{\sqrt{2}}\ ]^\top \tag{50c}$$
$$\mathcal{N}_{\mathcal{F}_4} = [\ -1 \quad 0\ ]^\top \tag{50d}$$
$$\mathcal{N}_{\mathcal{F}_5} = [\ -\tfrac{1}{\sqrt{2}} \quad -\tfrac{1}{\sqrt{2}}\ ]^\top \tag{50e}$$
$$\mathcal{N}_{\mathcal{F}_6} = [\ 0 \quad -1\ ]^\top \tag{50f}$$
$$\mathcal{N}_{\mathcal{F}_7} = [\ \tfrac{1}{\sqrt{2}} \quad -\tfrac{1}{\sqrt{2}}\ ]^\top \tag{50g}$$
$$\mathcal{N}_{\mathcal{F}_8} = [\ 1 \quad 0\ ]^\top \tag{50h}$$

Again, the polytope being 2-dimensional, it is a simple polytope, moreover $\text{ind}(\mathcal{V}_1) = \{\mathcal{F}_8, \mathcal{F}_1\}$ and for

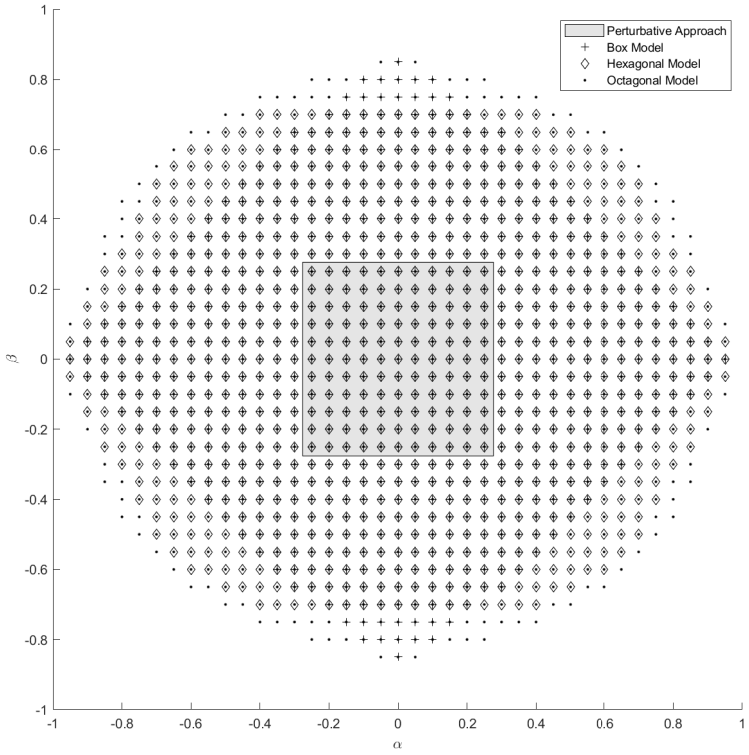

Figure 8: Stability (α, β)-regions of (11) using Theorem 4.2 on the T-S models (53) (octagonal model), (48) (hexagonal model), (43) (box model), and using the perturbative approach of Section 3.2

all $i \in [\![2, 8]\!]$, $\mathrm{ind}(\mathcal{V}_i) = \{\mathcal{F}_{i-1}, \mathcal{F}_i\}$. The weight functions are computed using Lemma 4.1:

$$w_{\mathcal{V}_1}(\theta) = \frac{1}{(1-\theta_1)(\sqrt{2}-\theta_1-\theta_2)} \tag{51a}$$

$$w_{\mathcal{V}_2}(\theta) = \frac{1}{(1-\theta_2)(\sqrt{2}-\theta_1-\theta_2)} \tag{51b}$$

$$w_{\mathcal{V}_3}(\theta) = \frac{1}{(1-\theta_2)(\sqrt{2}+\theta_1-\theta_2)} \tag{51c}$$

$$w_{\mathcal{V}_4}(\theta) = \frac{1}{(1+\theta_1)(\sqrt{2}+\theta_1-\theta_2)} \tag{51d}$$

$$w_{\mathcal{V}_5}(\theta) = \frac{1}{(1+\theta_1)(\sqrt{2}+\theta_1+\theta_2)} \tag{51e}$$

$$w_{\mathcal{V}_6}(\theta) = \frac{1}{(1+\theta_2)(\sqrt{2}+\theta_1+\theta_2)} \tag{51f}$$

$$w_{\mathcal{V}_7}(\theta) = \frac{1}{(1+\theta_2)(\sqrt{2}-\theta_1+\theta_2)} \tag{51g}$$

$$w_{\mathcal{V}_8}(\theta) = \frac{1}{(1-\theta_1)(\sqrt{2}-\theta_1+\theta_2)} \tag{51h}$$

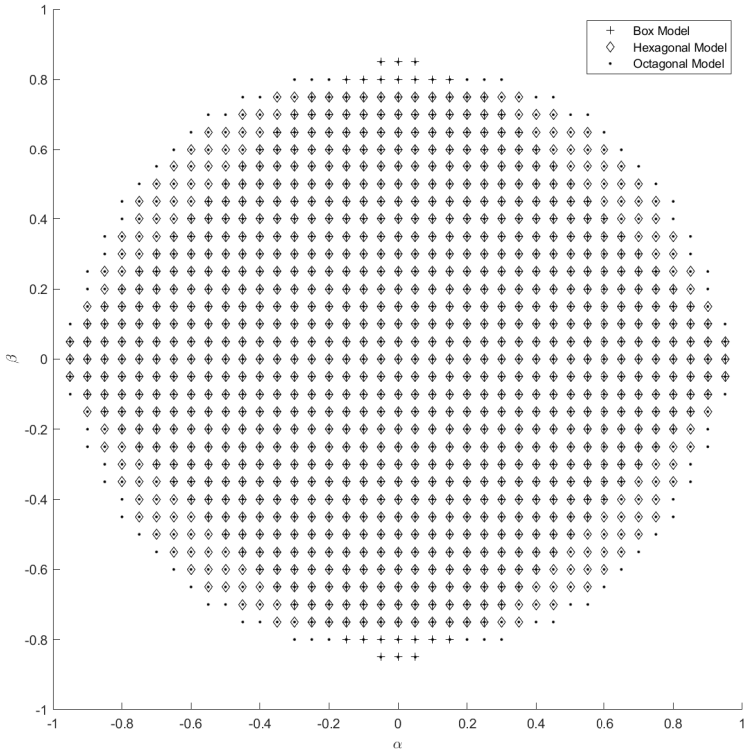

Figure 9: Stability (α, β)-regions of (11) using the piecewise quadratic Lyapunov function of [38] on the T-S models (53) (octagonal model), (48) (hexagonal model), (43) (box model)

which provides the barycentric coordinates of θ within the octagon Ω:

$$h_{\mathcal{V}_1}(\theta) = \frac{(\theta_2^2-1)(\theta_1+1)(\theta_1+\theta_2+\sqrt{2})(-(\theta_1-\theta_2)^2+2)}{4(\theta_1^2+\theta_2^2-2)(2\sqrt{2}+(1-\sqrt{2})\theta_1^2+(1-\sqrt{2})\theta_2^2)} \tag{52a}$$

$$h_{\mathcal{V}_2}(\theta) = \frac{(\theta_1^2-1)(\theta_2+1)(\theta_1+\theta_2+\sqrt{2})(-(\theta_1-\theta_2)^2+2)}{4(\theta_1^2+\theta_2^2-2)(2\sqrt{2}+(1-\sqrt{2})\theta_1^2+(1-\sqrt{2})\theta_2^2)} \tag{52b}$$

$$h_{\mathcal{V}_3}(\theta) = \frac{(\theta_1^2-1)(\theta_2+1)(\theta_1-\theta_2-\sqrt{2})((\theta_1+\theta_2)^2-2)}{4(\theta_1^2+\theta_2^2-2)(2\sqrt{2}+(1-\sqrt{2})\theta_1^2+(1-\sqrt{2})\theta_2^2)} \tag{52c}$$

$$h_{\mathcal{V}_4}(\theta) = \frac{(\theta_2^2-1)(\theta_1-1)(-\theta_1+\theta_2+\sqrt{2})((\theta_1+\theta_2)^2-2)}{4(\theta_1^2+\theta_2^2-2)(2\sqrt{2}+(1-\sqrt{2})\theta_1^2+(1-\sqrt{2})\theta_2^2)} \tag{52d}$$

$$h_{\mathcal{V}_5}(\theta) = \frac{(\theta_2^2-1)(\theta_1-1)(\theta_1+\theta_2-\sqrt{2})(-(\theta_1-\theta_2)^2+2)}{4(\theta_1^2+\theta_2^2-2)(2\sqrt{2}+(1-\sqrt{2})\theta_1^2+(1-\sqrt{2})\theta_2^2)} \tag{52e}$$

$$h_{\mathcal{V}_6}(\theta) = \frac{(\theta_1^2-1)(\theta_2-1)(\theta_1+\theta_2-\sqrt{2})(-(\theta_1-\theta_2)^2+2)}{4(\theta_1^2+\theta_2^2-2)(2\sqrt{2}+(1-\sqrt{2})\theta_1^2+(1-\sqrt{2})\theta_2^2)} \tag{52f}$$

$$h_{\mathcal{V}_7}(\theta) = \frac{(\theta_1^2-1)(\theta_2-1)(\theta_1-\theta_2+\sqrt{2})((\theta_1+\theta_2)^2-2)}{4(\theta_1^2+\theta_2^2-2)(2\sqrt{2}+(1-\sqrt{2})\theta_1^2+(1-\sqrt{2})\theta_2^2)} \tag{52g}$$

$$h_{\mathcal{V}_8}(\theta) = \frac{(\theta_2^2-1)(\theta_1+1)(-\theta_1+\theta_2-\sqrt{2})((\theta_1+\theta_2)^2-2)}{4(\theta_1^2+\theta_2^2-2)(2\sqrt{2}+(1-\sqrt{2})\theta_1^2+(1-\sqrt{2})\theta_2^2)} \tag{52h}$$

Finally, the NLSA on the polytope Ω is completed and the system (12) is exactly represented by the following

T-S model:

$$\dot{x}(t) = \sum_{i=1}^{8} h_{\mathcal{V}_i}(\theta) A(\mathcal{V}_i) x(t) \tag{53}$$

The stability analysis of the T-S model (53) is performed using Theorem 4.2 at several $(\alpha, \beta) \in \mathbb{R}^2$ values. The (α, β)-region for which the system (53) (octagonal model) is found to be stable is plotted on Figure 8, where it is compared to the (α, β)-region obtained with the T-S models (48) (hexagonal model), (43) (box model), and with the perturbative approach of Section 3.2. The (α, β)-region of stability is visibly larger by using Theorem 4.2 on the T-S model (53) (octagonal model) than on the two other T-S models: indeed, the octagonal bounding set is sharper than the box-shaped and hexagonal bounding sets, which relaxes the conservatism of the stability analysis.

Remark 4.2. *In order to show that using a more sophisticated Lyapunov function does not change which models perform better than the others, the piecewise quadratic Lyapunov function of [38] is now used in the stability analysis of the three T-S models. Using $\tau_{i,i,k} = 0$ and $\tau_{i,j,k} = 1$ $(i \neq j)$ for all models in the LMI conditions found in Theorem 1 of [38], the (α, β)-regions for which the T-S models (53) (octagonal model), (48) (hexagonal model) and (43) (box model) are found to be stable are plotted on Figure 9. As expected, all the (α, β)-regions of stability are larger than on Figure 8, and the octagonal model still outperforms the hexagonal model, this latter also outperforming the box model.*

Remark 4.3. *So far, the conservatism reduction has only been achieved by accumulating more and more local models in the T-S representation. This is due to the nonlinearities of the toy model which are shaped like a circle, and this accumulation is not an essential feature of the polytopic NLSA. Indeed, applying the polytopic NLSA to the T-S model described in [48] after its useless vertices have been removed can diminish the number of local models from $n_\Omega = 2^{n_\theta}$ to $n_\Omega = n_\theta + 1$. As shown in [48], getting rid of the useless vertices of this system reduces the conservatism of the controller design problem.*

5. The NLSA for Smooth Convex Sets

This section introduces a new NLSA for smooth convex sets, i.e. when the scheduling vector θ is bounded within a convex set Ω with a smooth boundary $\mathcal{S}_\Omega$. Lemma 5.1 provides the barycentric coordinates of θ inside Ω. Following the procedure of the NLSA, Theorem 5.1 uses these barycentric coordinates as weighting functions in order to obtain a new kind of T-S model, where the discrete sum is replaced by an integral along $\mathcal{S}_\Omega$, and which exactly represents (1) for all $\theta \in \Omega$. After discussing the advantages and inconveniences of the NLSA on a smooth convex set, basic results of stability for the newly introduced T-S-like models are provided, followed by an application of these results to the nonlinear system (11) of Section 3.2.

5.1. NLSA method

Lemma 5.1 (Barycentric coordinates of a Smooth Convex Set)**.** *Let $\theta \in \mathbb{R}^{n_\theta}$ be bounded by the smooth and bounded convex set Ω whose boundary is a $(n_\theta - 1)$-dimensional smooth manifold denoted by $\mathcal{S}_\Omega$. For all $\mathcal{V} \in \mathcal{S}_\Omega$, $w_\mathcal{V}$ stands for the weight function associated to $\mathcal{V}$, with*

$$w_\mathcal{V}(\theta) = \frac{\kappa(\mathcal{V})}{\langle \mathcal{N}_\mathcal{V} | \mathcal{V} - \theta \rangle^{n_\theta}} \tag{54}$$

where $\kappa(\mathcal{V})$ represents the Gaussian curvature of $\mathcal{S}_\Omega$ at $\mathcal{V}$. The barycentric coordinates of θ in Ω are given by the functions $(h_\mathcal{V})_{\mathcal{V} \in \mathcal{S}_\Omega}$, obtained by a normalization of the previous weights, and defined for all $\mathcal{V} \in \mathcal{S}_\Omega$ by

$$h_\mathcal{V}(\theta) = \frac{w_\mathcal{V}(\theta)}{\int\limits_{\mathcal{W} \in \mathcal{S}_\Omega} w_\mathcal{W}(\theta) d\mathcal{S}_\Omega} \tag{55}$$

Proof. The three axioms for barycentric coordinates (3), (4), (6) are verified under their integral form, which can be found in [27]. The proof of the linear precision property can be found in [27] as well, and the two other properties are trivial by construction. □

Remark 5.1 (Expression of the Gaussian curvature [64])**.** *If there exists a smooth function* $f : \mathbb{R}^{n_\theta} \mapsto \mathbb{R}$ *such that*

$$\mathcal{S}_\Omega = \{\mathcal{V} \in \mathbb{R}^{n_\theta} : f(\mathcal{V}) = 0\} \tag{56}$$

then the Gaussian curvature of $\mathcal{S}_\Omega$ *at* $\mathcal{V}$ *can be expressed by*

$$\kappa(\mathcal{V}) = \frac{\nabla f(\mathcal{V}) H f^\top(\mathcal{V}) \nabla f^\top(\mathcal{V})}{\|\nabla f(\mathcal{V})\|^{n_\theta+1}} \tag{57}$$

where $\nabla f(\mathcal{V})$ *and* $Hf(\mathcal{V})$ *stand resp. for the gradient and for the Hessian of* f *at* $\mathcal{V}$*.*

Keeping the notations of Lemma 5.1, the following generalization of the NLSA on a smooth convex set can be stated.

Theorem 5.1 (NLSA on a Smooth Convex Set)**.** *The T-S-like model* (58) *is an exact representation of the nonlinear system* (1) *for all* $x(t)$*,* $u(t)$*,* $\sigma(t)$ *and* t *such that* $\theta \in \Omega$*.*

$$\delta x(t) = \int_{\mathcal{V} \in \mathcal{S}_\Omega} h_{\mathcal{V}}(\theta) \left[A(\mathcal{V})x(t) + B(\mathcal{V})u(t) + \alpha(\mathcal{V})\right] d\mathcal{S}_\Omega \tag{58a}$$

$$y(t) = \int_{\mathcal{V} \in \mathcal{S}_\Omega} h_{\mathcal{V}}(\theta) \left[C(\mathcal{V})x(t) + D(\mathcal{V})u(t) + \beta(\mathcal{V})\right] d\mathcal{S}_\Omega \tag{58b}$$

This NLSA approach and its resulting T-S-like model have never been studied in the literature before, and there are still no known method to extract computable LMI conditions from the stability analysis of such systems. If this T-S-like model is geometrically one of the sharpest convex representation of a nonlinear system presenting "smoothly" interdependent scheduling parameters, this is counterbalanced by the number of vertices $\mathcal{V} \in \mathcal{S}_\Omega$ which is infinite and uncountable, leading to a tricky stability analysis of such models. Some elementary results are given below in order to deal with the stability analysis of this T-S-like model using a QLF. Moreover, bounding interdependent nonlinearities within a smooth convex set Ω is a difficult problem in general with no systematic solution. However, this problem is well-studied if the class of smooth convex sets is restricted to ellipsoids, and it simply consists in finding the minimum volume ellipsoid which covers all the obtainable scheduling parameters θ (eventually after sampling them): the reader is referred to Section 8.4 of [65] for more details. In general, this NLSA seems to only be advantageous in highly circumstantial cases compared to the other approaches of this paper. Similarly to what was stated at the end of the Section 4.1, the computation of the continuous weight functions of the model involves some divisions by zero which have to be taken care of numerically, for example in Parallel Distributed Compensation (PDC) schemes.

5.2. Stability Analysis

Introducing a QLF to perform the stability analysis of the continuous-time and input-free T-S-like model (59) obtained via Theorem 5.1 is immediately problematic.

$$\dot{x}(t) = \int_{\mathcal{V} \in \mathcal{S}_\Omega} h_{\mathcal{V}}(\theta) A(\mathcal{V}) x(t) d\mathcal{S}_\Omega \tag{59}$$

Indeed, the LMI conditions stated below, which are the straightforward generalization of the LMI conditions found in Theorem 4.2, are often numerically intractable.

Theorem 5.2 (Quadratic Stability). *The T-S-like model (59) is globally exponentially stable if there exists $P = P^\top \in \mathbb{R}^{n_x \times n_x}$ such that the LMI conditions (60) are satisfied.*

$$P \succ 0 \tag{60a}$$
$$\forall \mathcal{V} \in \mathcal{S}_\Omega,\ \mathcal{H}(PA(\mathcal{V})) \prec 0 \tag{60b}$$

Proof. By convexity, the proof of this result is similar to the proof of Theorem 4.2. □

In particular, when Ω is an ellipsoid, i.e. when $\Omega = \mathcal{E}$ with $\mathcal{E}$ defined in (61), the problem of finding such a P is NP-hard.

$$\mathcal{E} = \left\{\theta \in \mathbb{R}^{n_\theta} : \theta^\top Q \theta \leq 1\right\} \text{ with } Q = Q^\top \succ 0 \tag{61}$$

Indeed, given $P = P^\top \in \mathbb{R}^{n_x \times n_x}$ and Ω an ellipsoid, simply checking if the conditions (60) are satisfied or not can be turned into an NP-complete problem.

Theorem 5.3 (NP-hardness). *Let $\Omega = \mathcal{E}$ where $\mathcal{E}$ is the ellipsoid defined in (61). Finding $P = P^\top \in \mathbb{R}^{n_x \times n_x}$ such that the LMI conditions (60) are satisfied is an NP-hard problem.*

Proof. $\mathcal{V} \in \mathcal{S}_\Omega$ is equivalent to the existence of $v \in \mathbb{R}^{n_\theta}$ such that

$$\begin{cases} v^\top v = 1 \\ \mathcal{V} = Q^{-\frac{1}{2}} v \end{cases} \tag{62}$$

By construction of the T-S model (see (9)), for all $\mathcal{V} \in \mathcal{S}_\Omega$

$$A(\mathcal{V}) = A_0 + \sum_{i=1}^{n_\theta} \left(Q^{-\frac{1}{2}} v\right)_{(i)} A_i \tag{63}$$

hence:

$$A(\mathcal{V}) = A_0 + \sum_{i=1}^{n_\theta} \left(\sum_{j=1}^{n_\theta} Q^{-\frac{1}{2}}_{(i,j)} v_{(j)} \right) A_i \tag{64}$$

which can be re-written as

$$A(\mathcal{V}) = A_0 + \sum_{j=1}^{n_\theta} v_{(j)} R_j \tag{65}$$

with $R_j = \sum_{i=1}^{n_\theta} Q^{-\frac{1}{2}}_{(i,j)} A_i$. Hence, the LMI condition (60b) is equivalent to the following condition:

$$\forall v \in \mathbb{R}^{n_\theta} : v^\top v = 1,\ \mathcal{H}\left(P \left(A_0 + \sum_{j=1}^{n_\theta} v_{(j)} R_j \right) \right) \prec 0 \tag{66}$$

Checking the LMI above for a given $P = P^\top \succ 0$ can be turned into NP-complete problem, as shown in Section 3.4.1 of [66], hence, finding P satisfying the previous LMI condition is an NP-hard problem. □

However, in spite of this pessimistic result, two tractable optimization problems are given to perform the stability analysis of the T-S-like model (59) when Ω is bounded by an ellipsoid $\mathcal{E}$. The first one introduces some conservatism in (60b) (Theorem 5.4). The second one relies on the structure of the state matrix, where it is assumed that the scheduling vector θ acts on a single column or row of $A(\theta)$ (Theorem 5.5).

Theorem 5.4 (The "Universal" Conservative Conditions). *Let $\Omega \subseteq \mathcal{E}$ where $\mathcal{E}$ is the ellipsoid defined in (61). By construction of the T-S-like model (59), for all $\theta \in \mathcal{E}$, $A(\theta)$ can be re-written as*

$$A(\theta) = A_0 + \sum_{k=1}^{n_\theta} v_{(k)}(\theta) R_k \tag{67}$$

with $v(\theta) \in \mathbb{R}^{n_\theta}$ *such that* $v^\top(\theta)v(\theta) \leq 1$ *and* $A_0, R_1, \ldots, R_{n_\theta} \in \mathbb{R}^{n_x \times n_x}$. *If there exists* $P = P^\top \in \mathbb{R}^{n_x \times n_x}$ *satisfying the LMI conditions*

$$P \succ 0 \tag{68a}$$

$$\begin{bmatrix} \mathcal{H}(PA_0) & \mathcal{H}(PR_1) & \mathcal{H}(PR_2) & \ldots & \mathcal{H}(PR_{n_\theta}) \\ \mathcal{H}(PR_1) & \mathcal{H}(PA_0) & 0 & \ldots & 0 \\ \mathcal{H}(PR_2) & 0 & \mathcal{H}(PA_0) & \ddots & \vdots \\ \vdots & \vdots & \ddots & \ddots & 0 \\ \mathcal{H}(PR_{n_\theta}) & 0 & \ldots & 0 & \mathcal{H}(PA_0) \end{bmatrix} \prec 0 \tag{68b}$$

then such a P *also satisfies* (60), *hence the T-S-like model* (59) *is globally exponentially stable.*

Proof. This is an application of the Theorem 3.4 of [66]. □

Theorem 5.5 (The "Rank 2" Conditions)**.** *It is assumed that the scheduling vector* θ *acts on the* l*-th column of* $A(\theta)$, *with* $l \in [\![1, n_x]\!]$. *Let* $\Omega \subseteq \mathcal{E}$ *where* $\mathcal{E}$ *is the ellipsoid defined in* (61). *By construction of the T-S model, for all* $\theta \in \mathcal{E}$, $A(\theta)$ *can be re-written as*

$$A(\theta) = A_0 + \sum_{k=1}^{n_\theta} v_{(k)}(\theta) r_k \tilde{e}_l^\top \tag{69}$$

with $\tilde{e}_l$ *the* l*-th column of* I_{n_x}, $v(\theta) \in \mathbb{R}^{n_\theta}$ *such that* $v^\top(\theta)v(\theta) \leq 1$, *and* $r_1, \ldots, r_{n_\theta} \in \mathbb{R}^{n_x}$. *In this case, there exists* $P = P^\top \in \mathbb{R}^{n_x \times n_x}$ *and* $\lambda \in \mathbb{R}_{>0}$ *satisfying the LMI conditions*

$$P \succ 0 \tag{70a}$$

$$\begin{bmatrix} \mathcal{H}(PA_0) + \lambda \tilde{e}_l \tilde{e}_l^\top & PR \\ R^\top P & -\lambda I_{n_x} \end{bmatrix} \prec 0 \tag{70b}$$

with $R = \begin{bmatrix} r_1 & \ldots & r_{n_\theta} \end{bmatrix}$ *if and only if this* P *also satisfies* (60), *which provides the global exponential stability of the T-S-like model* (59).

Proof. For all $\theta \in \mathcal{E}$, there exists $v(\theta) \in \mathbb{R}^{n_\theta}$ such that $\|v(\theta)\|_2 \leq 1$ and

$$A(\theta) = A_0 + Rv(\theta)\tilde{e}_l^\top \tag{71}$$

hence, when the scheduling vector θ acts on a single column of $A(\theta)$, (59) can be interpreted as a particular Norm Bound Linear Differential Inclusion (NLDI) system, and the LMI conditions demonstrating the stability of such systems are given in Section 5.1 of [12]. In this peculiar case, the equivalence between the LMI conditions (70) and (60) is found in Proposition 3.1 of [66]. □

Corollary 5.1. *The LMI conditions* (60) *also demonstrate the stability of the T-S-like model*

$$\dot{x}(t) = \int_{\mathcal{V} \in \mathcal{S}_\Omega} h_{\mathcal{V}}(\theta) A^\top(\mathcal{V}) x(t) d\mathcal{S}_\Omega \tag{72}$$

hence, it is also possible to use the LMI conditions (70) *when the scheduling vector* θ *acts on a single row of* $A(\theta)$, *instead of on a single column.*

Proof. Succinctly, if there exists P such that the LMI conditions (60) hold, then the LMI conditions (73) also hold by congruence.

$$P^{-1} \succ 0 \tag{73a}$$

$$\forall \mathcal{V} \in \mathcal{S}_\Omega, \ \mathcal{H}(A(\mathcal{V})P^{-1}) \prec 0 \tag{73b}$$

Hence there exists $P^{-1} \succ 0$ such that for all $\mathcal{V} \in \mathcal{S}_\Omega$, $\mathcal{H}(P^{-1}A^\top(\mathcal{V})) \prec 0$. □

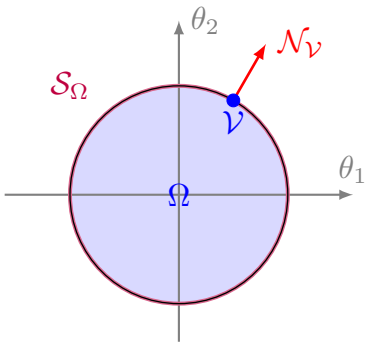

Figure 10: The disc Ω is bounding the scheduling vector θ of (13)

Remark 5.2. *The name of Theorems 5.4 and 5.5 are taken from [66].*

Leaving the quadratic framework, the natural generalization of the multiquadratic Lyapunov function is given by

$$V(x) = x^\top \left(\int_{\mathcal{V} \in \mathcal{S}_\Omega} h_\mathcal{V}(\theta) P(\mathcal{V}) d\mathcal{S}_\Omega \right) x \tag{74}$$

with for all $\mathcal{V} \in \mathcal{S}_\Omega$, $P(\mathcal{V}) = P^\top(\mathcal{V}) \succ 0$. The question of whether there exist tractable optimization problems to check the stability of the T-S-like model (59) by leveraging this multiquadratic Lyapunov function remains open for future works.

5.3. Application

Considering the LPV model (13), the disc $\Omega = \left\{\theta \in \mathbb{R}^2 : \theta_1^2 + \theta_2^2 \leq 1\right\}$ is chosen to be the bounding set of θ, as illustrated by Figure 10. The Gaussian curvature of a circle is constant and given by the inverse of its radius, and for all $\mathcal{V} \in \mathcal{S}_\Omega$, $\mathcal{N}_\mathcal{V} = \mathcal{V}$. The weight functions are computed using Lemma 5.1:

$$\begin{aligned} w_\mathcal{V}(\theta) =& \frac{1}{\left(\mathcal{V}_{(1)}(\mathcal{V}_{(1)} - \theta_1) + \mathcal{V}_{(2)}(\mathcal{V}_{(2)} - \theta_2)\right)^2} \\ =& \frac{1}{\left(1 - \mathcal{V}_{(1)}\theta_1 - \mathcal{V}_{(2)}\theta_2\right)^2} \end{aligned} \tag{75}$$

moreover, the following is verified [27]:

$$\int_{\mathcal{V} \in \mathcal{S}_\Omega} w_\mathcal{V}(\theta) d\mathcal{S}_\Omega = \frac{2\pi}{(1 - \theta_1^2 - \theta_2^2)^{3/2}} \tag{76}$$

which provides the barycentric coordinates of θ within the disc Ω:

$$h_\mathcal{V}(\theta) = \frac{(1 - \theta_1^2 - \theta_2^2)^{3/2}}{2\pi \left(1 - \mathcal{V}_{(1)}\theta_1 - \mathcal{V}_{(2)}\theta_2\right)^2} \tag{77}$$

Finally, the NLSA on the disc Ω is completed and the system (12) is exactly represented by the following T-S-like model:

$$\dot{x}(t) = \int_{\mathcal{V} \in \mathcal{S}_\Omega} h_\mathcal{V}(\theta) A(\mathcal{V}) x(t) d\mathcal{S}_\Omega \tag{78}$$

The stability analysis of the T-S-like model (78) is performed using Theorem 5.4 and Theorem 5.5 (which is applicable since θ acts on a single row of $A(\theta)$ in (13)) at several $(\alpha, \beta) \in \mathbb{R}^2$ values. The (α, β)-regions for which the system (78) (disc model) is found to be stable are plotted on Figure 11, where they are

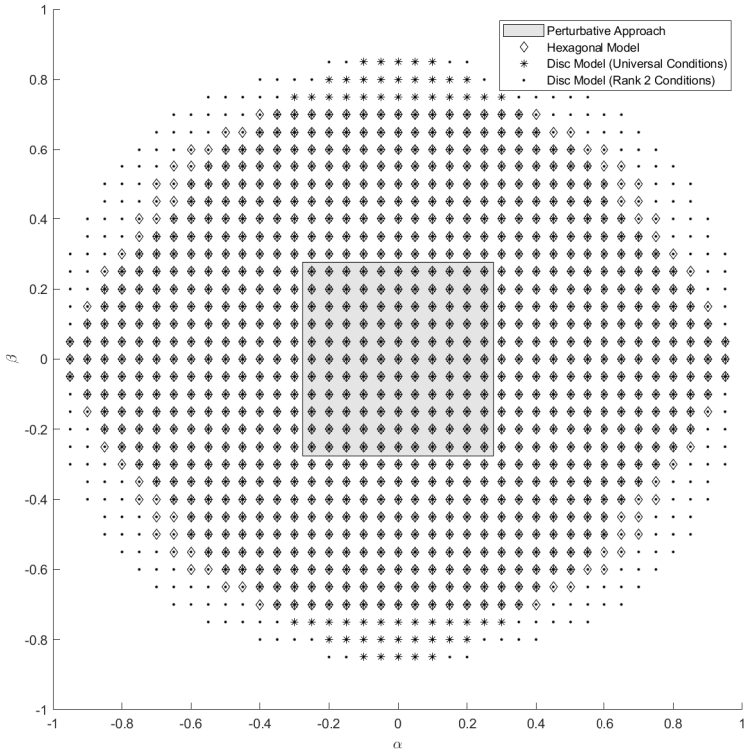

Figure 11: Stability (α, β)-regions of (11) using Theorem 5.4 ("universal" conditions) and Theorem 5.5 ("rank 2" conditions) on the T-S-like model (78) (disc model), using Theorem 4.2 on the T-S model (48) (hexagonal model), and using the perturbative approach of Section 3.2

compared to the (α, β)-regions obtained with the hexagonal T-S model (48) and the perturbative approach of Section 3.2. The (α, β)-region of stability is visibly larger by using Theorem 5.5 ("rank 2" conditions) instead of Theorem 5.4 ("universal" conditions) on the T-S-like model (78), which confirms that the "rank 2" LMI conditions are less conservative than the "universal" LMI conditions. Moreover, the (α, β)-region of stability for the hexagonal T-S model (48) is about the same size as the region computed on the T-S-like model (78) with Theorem 5.4, which indicates that, to some degree, the sharpness of the smooth convex shape has compensated the conservatism introduced by the "universal" LMI conditions. However, when these "universal" LMI conditions are compared to the stability results obtained using the T-S model (53) (octagonal model) on Figure 12, the conservatism introduced in the stability analysis is not compensated by the sharpness of the smooth convex shape anymore. Nevertheless, in all cases, the "rank 2" conditions outperform the others. This indicates that the NLSA for smooth convex shape seems to only be advantageous in highly circumstantial cases, e.g. when θ acts on a single row (or column) of $A(\theta)$.

6. Conclusion and Perspectives

The Nonlinear Sector Approach (NLSA) is a way to construct Takagi-Sugeno (T-S) models which exactly represent nonlinear systems whose nonlinearities are bounded by a box-shaped set. This paper has generalized the NLSA for larger classes of convex bounding sets: extending it for polytopic and smooth convex sets. These generalizations provide new ways of reducing the intrinsic conservatism of T-S representations with interdependent scheduling parameters, which has been demonstrated numerically through the study of simple Linear Matrix Inequalities (LMI) criteria for stability analysis of the resulting models. In particular, it has been shown that the LMI criteria for the newly introduced T-S-like models are still conservative, and the problem of stability and stabilization for these models is left open for further investigations. The NLSA

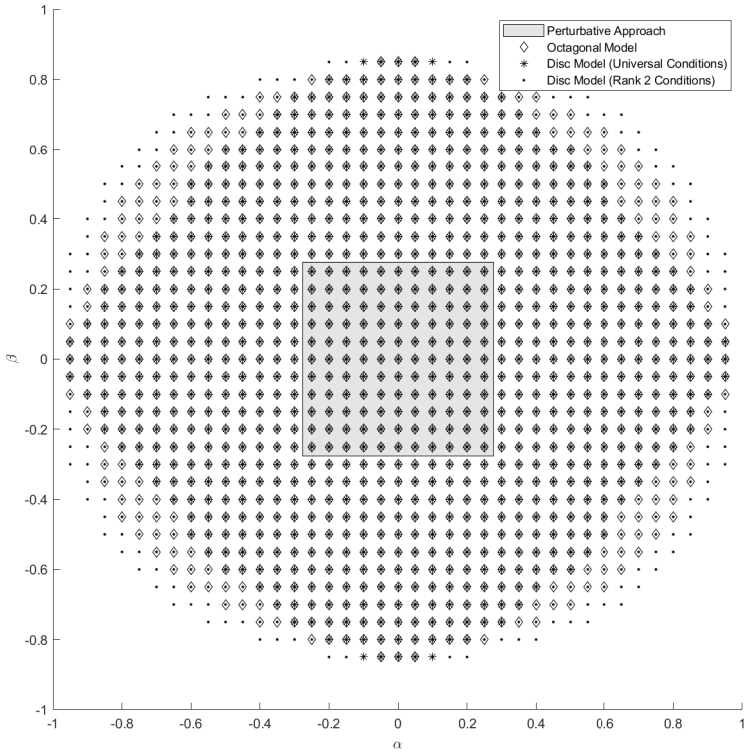

Figure 12: Stability (α, β)-regions of (11) using Theorem 5.4 ("universal" conditions) and Theorem 5.5 ("rank 2" conditions) on the T-S-like model (78) (disc model), using Theorem 4.2 on the T-S model (53) (octagonal model), and using the perturbative approach of Section 3.2

also remains to be extended for non-convex bounding sets, for example by exactly rewriting the nonlinear system as a switched T-S model on several polytopic sets arranged in a non-convex disposition.

References

[1] K. J. Astrom, R. M. Murray, Feedback systems: An Introduction for Scientists and Engineers, Princeton University Press, Princeton, NJ, 2008.

[2] P. A. Iglesias, B. P. Ingalls (Eds.), Control theory and systems biology, MIT Press, London, England, 2009.

[3] M. Lines (Ed.), Nonlinear Dynamical Systems in Economics, Springer Vienna, 2005. doi:10.1007/3-211-38043-4.

[4] G. G. Rigatos, State-Space Approaches for Modelling and Control in Financial Engineering, Springer International Publishing, 2017. doi:10.1007/978-3-319-52866-3.

[5] T. Takagi, M. Sugeno, Fuzzy identification of systems and its applications to modeling and control, IEEE Transactions on Systems, Man, and Cybernetics SMC-15 (1) (1985) 116–132. doi:10.1109/tsmc.1985.6313399.

[6] R. Murray-Smith, T. A. J. (Eds.), Multiple Model Approaches to Modelling and Control, Taylor and Francis, London, 1997.

[7] J. Shamma, M. Athans, Analysis of gain scheduled control for nonlinear plants, IEEE Transactions on Automatic Control 35 (8) (1990) 898–907. doi:10.1109/9.58498.

[8] Angelis, GZ (Georgo), System analysis, modelling and control with polytopic linear models (2001). doi:10.6100/IR541022.

[9] M. Bernal, A. Sala, Z. Lendek, T. M. Guerra, Problems to be solved and scope of the book, in: Analysis and Synthesis of Nonlinear Control Systems, Springer International Publishing, 2022, pp. 5–21. doi:10.1007/978-3-030-90773-0_2.

[10] P. Baranyi, The generalized TP model transformation for T-S fuzzy model manipulation and generalized stability verification, IEEE Transactions on Fuzzy Systems 22 (4) (2014) 934–948. doi:10.1109/tfuzz.2013.2278982.

[11] H.-K. Lam, Polynomial Fuzzy Model-Based Control Systems, Springer International Publishing, 2016. doi:10.1007/978-3-319-34094-4.

[12] S. Boyd, L. El Ghaoui, E. Feron, V. Balakrishnan, Linear Matrix Inequalities in System and Control Theory, Vol. 15 of Studies in Applied Mathematics, SIAM, Philadelphia, PA, 1994.

[13] K. Tanaka, H. O. Wang, Fuzzy Control Systems Design and Analysis, John Wiley & Sons, Inc., 2001. doi:10.1002/0471224596.

[14] M. Bernal, A. Sala, Z. Lendek, T. M. Guerra, Modelling via convex structures, in: Analysis and Synthesis of Nonlinear Control Systems, Springer International Publishing, 2022, pp. 23–96. doi:10.1007/978-3-030-90773-0_3.
[15] J. Abonyi, R. Babuska, F. Szeifert, Modified Gath-Geva fuzzy clustering for identification of Takagi-Sugeno fuzzy models, IEEE Transactions on Systems, Man and Cybernetics, Part B (Cybernetics) 32 (5) (2002) 612–621. doi:10.1109/tsmcb.2002.1033180.
[16] T. Johansen, R. Babuska, Multiobjective identification of Takagi-Sugeno fuzzy models, IEEE Transactions on Fuzzy Systems 11 (6) (2003) 847–860. doi:10.1109/tfuzz.2003.819824.
[17] D. Kukolj, E. Levi, Identification of complex systems based on neural and Takagi-Sugeno fuzzy model, IEEE Transactions on Systems, Man and Cybernetics, Part B (Cybernetics) 34 (1) (2004) 272–282. doi:10.1109/tsmcb.2003.811119.
[18] P. Angelov, D. Filev, An approach to online identification of Takagi-Sugeno fuzzy models, IEEE Transactions on Systems, Man and Cybernetics, Part B (Cybernetics) 34 (1) (2004) 484–498. doi:10.1109/tsmcb.2003.817053.
[19] C. Li, J. Zhou, B. Fu, P. Kou, J. Xiao, T-S fuzzy model identification with a gravitational search-based hyperplane clustering algorithm, IEEE Transactions on Fuzzy Systems 20 (2) (2012) 305–317. doi:10.1109/tfuzz.2011.2173693.
[20] M. Luo, F. Sun, H. Liu, Hierarchical structured sparse representation for T-S fuzzy systems identification, IEEE Transactions on Fuzzy Systems 21 (6) (2013) 1032–1043. doi:10.1109/tfuzz.2013.2240690.
[21] S.-H. Tsai, Y.-W. Chen, A novel identification method for Takagi-Sugeno fuzzy model, Fuzzy Sets and Systems 338 (2018) 117–135. doi:10.1016/j.fss.2017.10.012.
[22] T. Johansen, R. Shorten, R. Murray-Smith, On the interpretation and identification of dynamic Takagi-Sugeno fuzzy models, IEEE Transactions on Fuzzy Systems 8 (3) (2000) 297–313. doi:10.1109/91.855918.
[23] K. Kiriakidis, Nonlinear modeling by interpolation between linear dynamics and its application in control, Journal of Dynamic Systems, Measurement, and Control 129 (6) (2007) 813–824. doi:10.1115/1.2789473.
[24] H. Ohtake, K. Tanaka, H. Wang, Fuzzy modeling via sector nonlinearity concept, in: Proceedings Joint 9th IFSA World Congress and 20th NAFIPS International Conference (Cat. No. 01TH8569), IEEE, 2001. doi:10.1109/nafips.2001.944239.
[25] A. P. White, G. Zhu, J. Choi, Linear Parameter-Varying Control for Engineering Applications, Springer London, 2013. doi:10.1007/978-1-4471-5040-4.
[26] S. Bezzaoucha, B. Marx, D. Maquin, J. Ragot, State and parameter estimation for time-varying systems: a Takagi-Sugeno approach, IFAC Proceedings Volumes 46 (2) (2013) 761–766. doi:10.3182/20130204-3-fr-2033.00106.
[27] J. Warren, S. Schaefer, A. N. Hirani, M. Desbrun, Barycentric coordinates for convex sets, Advances in Computational Mathematics 27 (3) (2006) 319–338. doi:10.1007/s10444-005-9008-6.
[28] C. Hoffmann, H. Werner, Complexity of implementation and synthesis in linear parameter-varying control, IFAC Proceedings Volumes 47 (3) (2014) 11749–11760. doi:10.3182/20140824-6-za-1003.00617.
[29] H. Ohtake, K. Tanaka, H. Wang, Polar coordinate fuzzy model and stability analysis, in: Proceedings of the 2003 American Control Conference, 2003., IEEE. doi:10.1109/acc.2003.1243353.
[30] K. Tanaka, H. Yoshida, H. Ohtake, H. Wang, A sum-of-squares approach to modeling and control of nonlinear dynamical systems with polynomial fuzzy systems, IEEE Transactions on Fuzzy Systems 17 (4) (2009) 911–922. doi:10.1109/tfuzz.2008.924341.
[31] S.-H. Yoo, B.-J. Choi, A balanced model reduction for T-S fuzzy systems with uncertain time varying parameters, in: Computational and Information Science, Springer Berlin Heidelberg, 2004, pp. 148–153. doi:10.1007/978-3-540-30497-5_24.
[32] L. Wu, X. Su, P. Shi, J. Qiu, Model approximation for discrete-time state-delay systems in the ts fuzzy framework, IEEE Transactions on Fuzzy Systems 19 (2) (2011) 366–378. doi:10.1109/tfuzz.2011.2104363.
[33] B. Marx, A descriptor Takagi-Sugeno approach to nonlinear model reduction, Linear Algebra and its Applications 479 (2015) 52–72. doi:10.1016/j.laa.2015.03.030.
[34] A. El-Amrani, B. Boukili, A. E. Hajjaji, A. Hmamed, H∞ model reduction for T-S fuzzy systems over finite frequency ranges, Optimal Control Applications and Methods 39 (4) (2018) 1479–1496. doi:10.1002/oca.2422.
[35] A. Kwiatkowski, LPV modeling and application of LPV controllers to SI engines, Ph.D. thesis (Nov. 2008).
[36] A. M. Nagy, G. Mourot, B. Marx, J. Ragot, G. Schutz, Systematic multimodeling methodology applied to an activated sludge reactor model, Industrial & Engineering Chemistry Research 49 (6) (2010) 2790–2799. doi:10.1021/ie8017687.
[37] M. Johansson, A. Rantzer, K.-E. Arzen, Piecewise quadratic stability of fuzzy systems, IEEE Transactions on Fuzzy Systems 7 (6) (1999) 713–722. doi:10.1109/91.811241.
[38] M. Chadli, D. Maquin, J. Ragot, Nonquadratic stability analysis of Takagi-Sugeno models, in: Proceedings of the 41st IEEE Conference on Decision and Control, IEEE, 2002. doi:10.1109/cdc.2002.1184847.
[39] K. Tanaka, T. Hori, H. Wang, A multiple Lyapunov function approach to stabilization of fuzzy control systems, IEEE Transactions on Fuzzy Systems 11 (4) (2003) 582–589. doi:10.1109/tfuzz.2003.814861.
[40] B.-J. Rhee, S. Won, A new fuzzy Lyapunov function approach for a Takagi-Sugeno fuzzy control system design, Fuzzy Sets and Systems 157 (9) (2006) 1211–1228. doi:10.1016/j.fss.2005.12.020.
[41] T. M. Guerra, A. Jaadari, J. Pan, A. Sala, Some refinements for non quadratic stabilization of continuous TS models, in: 2011 IEEE International Conference on Fuzzy Systems (FUZZ-IEEE 2011), IEEE, 2011. doi:10.1109/fuzzy.2011.6007569.
[42] A. Sala, C. Arino, Asymptotically necessary and sufficient conditions for stability and performance in fuzzy control: Applications of polya's theorem, Fuzzy Sets and Systems 158 (24) (2007) 2671–2686. doi:10.1016/j.fss.2007.06.016.
[43] A. Sala, C. Arino, Relaxed stability and performance LMI conditions for Takagi-Sugeno fuzzy systems with polynomial constraints on membership function shapes, IEEE Transactions on Fuzzy Systems 16 (5) (2008) 1328–1336. doi:10.1109/tfuzz.2008.926585.
[44] A. Kruszewski, R. Wang, T. M. Guerra, Nonquadratic stabilization conditions for a class of uncertain nonlinear discrete

time TS fuzzy models: A new approach, IEEE Transactions on Automatic Control 53 (2) (2008) 606–611. doi:10.1109/tac.2007.914278.
[45] M. Bernal, T. M. Guerra, A. Kruszewski, A membership-function-dependent approach for stability analysis and controller synthesis of Takagi-Sugeno models, Fuzzy Sets and Systems 160 (19) (2009) 2776–2795. doi:10.1016/j.fss.2009.02.005.
[46] L. Mozelli, R. Palhares, F. Souza, E. Mendes, Reducing conservativeness in recent stability conditions of TS fuzzy systems, Automatica 45 (6) (2009) 1580–1583. doi:10.1016/j.automatica.2009.02.023.
[47] A. Kruszewski, A. Sala, T. Guerra, C. Arino, A triangulation approach to asymptotically exact conditions for fuzzy summations, IEEE Transactions on Fuzzy Systems 17 (5) (2009) 985–994. doi:10.1109/tfuzz.2009.2019124.
[48] D. Robert, O. Sename, D. Simon, An H∞ LPV design for sampling varying controllers: Experimentation with a T-inverted pendulum, IEEE Transactions on Control Systems Technology 18 (3) (2010) 741–749. doi:10.1109/tcst.2009.2026179.
[49] F. Anstett, G. Millérioux, G. Bloch, Polytopic observer design for LPV systems based on minimal convex polytope finding, Journal of Algorithms & Computational Technology 3 (1) (2009) 23–43. doi:10.1260/174830109787186569.
[50] C. Hoffmann, Linear parameter-varying control of systems of high complexity, Regelungstechnik, Verlag Dr. Hut GmbH, Munich, Germany, 2016. doi:10.15480/882.1301.
[51] B. Grünbaum, Convex Polytopes, Springer New York, 2003. doi:10.1007/978-1-4613-0019-9.
[52] G. M. Ziegler, Lectures on Polytopes, Springer New York, 1995. doi:10.1007/978-1-4613-8431-1.
[53] J. Hauser, S. Sastry, G. Meyer, Nonlinear control design for slightly non-minimum phase systems: Application to V/STOL aircraft, Automatica 28 (4) (1992) 665–679. doi:10.1016/0005-1098(92)90029-f.
[54] L. Marconi, A. Isidori, A. Serrani, Autonomous vertical landing on an oscillating platform: an internal-model based approach, Automatica 38 (1) (2002) 21–32. doi:10.1016/s0005-1098(01)00184-4.
[55] A. D. Luca, G. Oriolo, M. Vendittelli, Control of wheeled mobile robots: An experimental overview, in: Ramsete, Springer Berlin Heidelberg, 2001, pp. 181–226. doi:10.1007/3-540-45000-9_8.
[56] H. K. Khalil, Nonlinear Systems, 3rd Edition, Pearson, Upper Saddle River, NJ, 2001.
[57] J. Warren, On the uniqueness of barycentric coordinates, in: Contemporary Mathematics, Proceedings of AGGM02, 2003. doi:10.1090/conm/334/05977.
[58] J. Warren, Barycentric coordinates for convex polytopes, Advances in Computational Mathematics 6 (1) (1996) 97–108. doi:10.1007/bf02127699.
[59] A. Sala, C. Arino, Relaxed stability and performance conditions for Takagi-Sugeno fuzzy systems with knowledge on membership function overlap, IEEE Transactions on Systems, Man and Cybernetics, Part B (Cybernetics) 37 (3) (2007) 727–732. doi:10.1109/tsmcb.2006.887949.
[60] F. P. Preparata, M. I. Shamos, Computational Geometry, Springer New York, 1985. doi:10.1007/978-1-4612-1098-6.
[61] G. Kalai, Linear programming, the simplex algorithm and simple polytopes, Mathematical Programming 79 (1-3) (1997) 217–233. doi:10.1007/bf02614318.
[62] H. Wang, K. Tanaka, M. Griffin, An approach to fuzzy control of nonlinear systems: stability and design issues, IEEE Transactions on Fuzzy Systems 4 (1) (1996) 14–23. doi:10.1109/91.481841.
[63] R. B. (auth.), Matrix Analysis, 1st Edition, Graduate Texts in Mathematics N°169, Springer, 1997.
[64] R. Goldman, Curvature formulas for implicit curves and surfaces, Computer Aided Geometric Design 22 (7) (2005) 632–658. doi:10.1016/j.cagd.2005.06.005.
[65] S. Boyd, L. Vandenberghe, Convex Optimization, Cambridge University Press, 2004. doi:10.1017/cbo9780511804441.
[66] A. Ben-Tal, A. Nemirovski, Robust convex optimization, Mathematics of Operations Research 23 (4) (1998) 769–805. doi:10.1287/moor.23.4.769.